CRITICAL STABILITY OF THE BERNSTEIN MODES FOR A HOLLOW DISTRIBUTION FUNCTION

by

R. St.Quinton

Thesis submitted for the degree of

Master of Philosophy

August 1973

Department of Physics

Imperial College

London, S. W. 7.

ABSTRACT

An investigation is carried out to obtain the necessary conditions for critical stability of the Bernstein modes in order to interpret the strong electrostatic emissions with frequencies near $(2n+1)\Omega/2$ predominantly detected in the magnetosphere in the night-side auroral L-shells.

It will be shown that for a given anisotropic distribution function of the form $f_0=g(\underline{v}-\underline{V})S(v_\perp)$, a non-resonant plasma instability can result.

It will be seen that instability occurs, within a given range of wavelengths and that unstable mode solutions are separated by bands in the wavelength where only stable mode solutions are possible.

It was further found that as $\lambda\to\infty$, only stable modes propagate, so it appears there is an upper limit in wavelength for instability to be possible.

Conversely as $\lambda\to 0$ fluctuations become so rapid that no fine structure remains. Also the critical plasma density for instability becomes infinite for sufficiently short wavelengths.

An analysis is carried out to determine the first $k_\perp$ for which the modes become unstable as various parameters of the distribution function change their value. For each unstable $k_\perp$ there corresponds a minimum critical plasma density below which instability is not possible.

The introduction contains a short review of some of the observational data conserning the wave-emissions with frequency $\sim 3/2\,\Omega$ and a discussion on the theory of Bernstein mo-

des. In chapters 1, II, III, IV and V the dispersion relation in the electrostatic approximation is derived, first for the general case where both $k_{\parallel}$ and $k_{\perp}$ are finite and then specialized for the case $k_{\parallel} = 0$, where Landau damping can be rigorously neglected and pure Bernstein modes of the higher frequency regime propagate. Then having chosen a particular distribution function we proceed to investigate the conditions for critical stability. Some observations on the particle populations in the night-side of the magnetosphere are included in support of the choice of the distribution function. Chapters VI and VII, consider the present results in the light of the available data and of previous research on this topic.

TABLE OF CONTENTS

ACKNOWLEDGEMENTS

I would like to thank Professor J.W.Dungey for suggesting the topic for this thesis, for his subsequent helpful advice and his continued forbearance. I would also like to thank D.T.Elliott for many helpful discussions on the computational problem.

INTRODUCTION

Extensive laboratory experiments and theoretical analysis show that waves play dominant roles in all non-equilibrium plasma systems. Especially when the plasma is dilute and hot, ordinary Coulomb collisions are unimportant and wave particle interactions govern the dynamics of the system.

The introduction of a finite temperature in the plasma gives rise to a type of mode characterised by a phase velocity which is slow compared to the cold plasma modes and by the direction of the electric field, $\underline{E}$, which turns out to be approximately parallel to the wave-vector, $\underline{k}$; $\underline{E}$ may then be derived from a scalar potential field and the mode is therefore called electrostatic. This mode has no counterpart in cold plasma.

The magnetosphere contains a great variety of particle populations, discussed by Vette (1972), where distributions almost at any point in space and time are non-equilibrium ones.

Until recently a great emphasis has been placed on the study of electromagnetic instabilities of the magnetosphere. It appears however from laboratory systems that electrostatic wave modes develop quite readily and when their phase velocity is comparable to the plasma thermal speed they can interact more strongly than the electromagnetic modes with the plasma.

Since March 1968 the OGO 5 plasma wave experiment has sampled a lot of characteristics of waves in the magnetosphere a general survey of which is given by Scarf and Fredricks (1972). Among them they have detected a form of electrostatic emissions that appear to interact very strongly with the local plasma particles. These large amplitude waves are well localized at $4 \leqslant L \leqslant 10$, MLAT $\leqslant 10^{o}$ and have frequencies (ω), about 3kHz.,corresponding to approximately 3/2 the gyrofrequency (Ω) of 80keV electrons. See figure (1). Their duration varies between minutes and at times hours.

Observations so far show a close correlation of these waves with magnetic substorms. The power in the $(3/2)\Omega$-wave increases by more than 5 orders of magnitude during substorm expansion which would suggest that the electric field emissions have enhanced amplitudes, that they locally interact with energetic electrons to produce local isotropy in the particle distributions and produce strong diffusion and particle

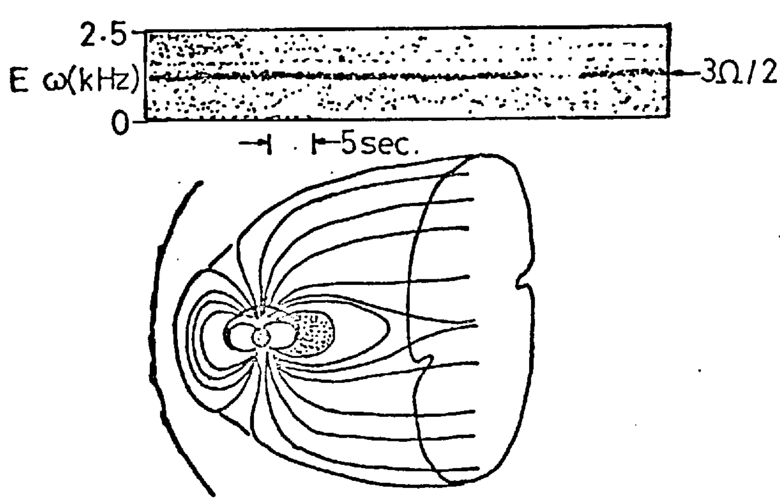

Figure(1)

Sketch of the magnetospheric cavity with the shaded area indicating the region where intense $(3/2)\Omega$ waves are observed and a characteristic frequency-time diagram of these waves based on OGO 5 observations.

(After Scarf and Fredricks 1972).

precipitation.

Their additional correlation with simultaneous but distant precipitation events on nearly the same L-shells seem to be supported also by other independent observations. Pilkington (1972) from balloon X-ray experiments and subsequent monitoring of the auroral electron spectrum in the midnight sector supports the idea that the $(3/2)\Omega$-waves could be responsible for the pitch-angle diffusion of kilovolt electrons.

Other measurements made by Evans (1968), on the precipitation zone of electrons with energies greater than 20keV at auroral zone latitudes near midnight and on electrons with $E > 40$keV indicate that with increasing magnetic activity the greatest relative increase in the spectrum occurs at some energy $\simeq 40$keV, see figure(2).

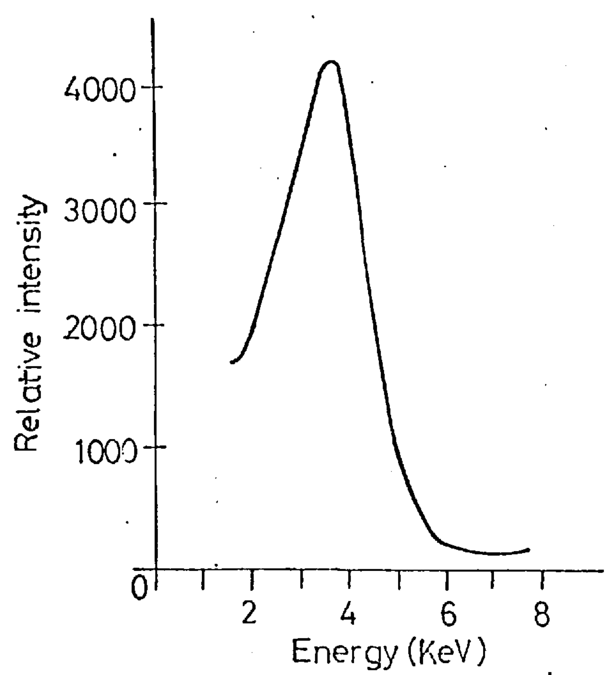

Figure(2)

Nearly monoenergetic electron spectrum measured in break-up aurora. (After Evans 1968).

They suggest that firstly a plasma instability is necessary to account for the high energy particles in aurora and secondly that only an electrostatic field would account for the nearly monoenergetic spectrum of the electrons in figure (2).

The electrostatic modes have been discussed in considerable detail by E.P.Gross (1951), G.V.Gordeyev, I.Bernstein (1958) and others. Because they are slow waves they are induced easily into overstability by an anisotropy in the particle velocity distribution. In this context they are discussed by E.G.Harris (1959, 1961).

Overstability is to be understood as the type of instability in which ω is complex rather than pure imaginary. Hereafter however, I shall use the term instability avoiding the above distinction.

To obtain the general dispersion relation in the electrostatic approximation various conditions have to be satisfied. These are discussed in some detail in chapter 1. Some general points however are worth mentioning.

To obtain the states of critical stability, i.e. the solutions of the dispersion relation for real ω and $\underline{k}$, the zero-damped dispersion relation must be obtained first. Having done so, it is then relatively easy to add the relevant parameters of anisotropy and examine the requirements for instability.

If $k_{\parallel}$ is finite the dispersion relation in the electrostatic approximation includes a term representing Landau damping which can only be neglected if various conditions are satisfied so that it may be assumed small. As it was mentioned before, electrostatic modes are due to finite temperatures of the electrons. As the electron temperature is lowered i.e. conditions approach those of a collision free cold plasma, the Landau damping of this mode increases reaching its maximum when the electron thermal speed is about equal to the wave phase velocity which is the vicinity where the real part of the K_{zz} element of the dielectric tensor passes through zero and becomes pure imaginary at which point the mode disappears completely; where z is the direction of the magnetic field.

A case in which, however, Landau damping may be rigorously neglected, occurs for propagation at angles of 90°, where $k_{\parallel} = 0$. The dispersion relation obtained under this condition yields solutions for purely electrostatic modes which were first described by I.Bernstein (1958).

The Bernstein modes are electrostatic waves of high frequency i.e. at frequencies which are various multiples of the ion and electron cyclotron frequencies, separated from each other by gaps in which strong cyclotron damping occurs. For waves with frequency in the region of the electron cyclotron frequency and above the ion contribution in the dispersion relation can be neglected since $(\omega/\Omega) \equiv w$ is so large. Solutions to the dispersion relation then appear only when F(w), refer to figure (III.3), is positive, which occurs on the high frequency side of the asymptotes $\omega = n\Omega$, $n \geqslant 1$. The lowest temperature Bernstein mode for this high frequency regime occurs at the upper hybrid resonant frequency $(\omega^2 = \Omega^2 + \omega_p^2)$, and solutions exist for arbitrary large λ.

Finally it is worth describing briefly what happens if $k_{\parallel}$ is finite. A qualitative plot of the function $F(w,\zeta)$, where $\zeta \equiv k_{\perp}/k_{\parallel}$, is illustrated in figure (3) and it can be seen that $F(w,\zeta)$ remains finite at the $w + n = 0$ points. For a definition of the function $F(w)$ refer to equation (III.7) and (III.8).

Moreover it can be seen from the plot in figure (3) that there is a decay in the amplitude of the successive oscillations of $F(w,\zeta)$ for large values of w. That implies that for $k_{\parallel} \neq 0$ the spectra of the electrostatic waves with frequencies above the electron and ion cyclotron frequencies will be bound in each case by a maximum frequency.

The Bernstein modes so far described are solutions of

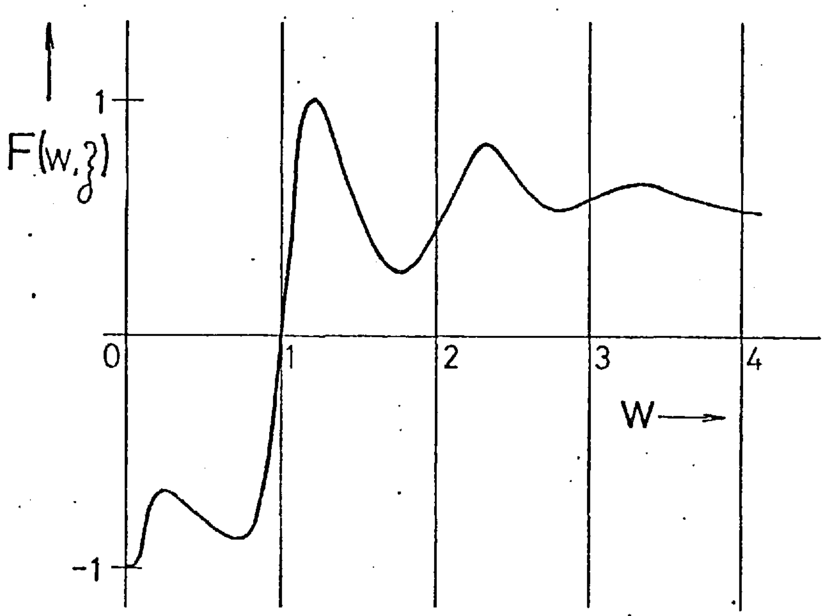

Figure (3)

Plot of $F(w,\zeta)$ versus w, describing the behaviour of modes in the electrostatic approximation, when $k_{\parallel}$ is finite the dispersion relation for a Maxwellian distribution function and represent stable undamped propagation.

In the present analysis solutions of the electrostatic dispersion relation are sought for an anisotropic distribution. It will be seen that this anisotropic distribution can lead to unstable solutions.

The analysis is for the zero-damped dispersion relation and investigates the necessary conditions for critical stability of the Bernstein modes i.e. of electrostatic waves propagating in a plane perpendicular to the magnetic field $\underline{B}_0$. It will be shown that the onset of instability occurs at $\omega \simeq (3/2)\Omega$ with a frequency spectrum between $1.4 \leqslant \omega/\Omega \leqslant 1.5$, which seems to be in agreement with observations, to be discussed at the end of this work.

(1).ELECTROSTATIC (SCALAR) DISPERSION RELATION.

The distinguishing characteristic of electrostatic waves is that the electric field may be derived from a potential and that $\underline{E}$ is parallel to $\underline{k}$ and hence the wave is longitudinal in nature.The electrostatic approximation is valid only if

$$|n^2| \gg |K_{ij}|$$

for all i and j; Where n is the refractive index, $\underline{n} = \underline{k}c/\omega$, and K is the dielectric tensor. The theory for this restriction is covered in the "Theory of Plasma Waves" by Stix (1962).

To obtain therefore the dispersion relation in the electrostatic approximation we must impose the restrictions that the wavelengths are short compared to the Larmor radii and the phase velocity is very much smaller than the velocity of light; a condition obtained directly from the above inequality and the definition of $\underline{n}$. For, as $|n|$ becomes very large this implies $(k/\omega) \ll c$.

Now,electrostatic modes are obtainable only as a result of finite temperatures of the electrons and have no counterpart in cold plasma. However, the introduction of finite temperatures need only impose minor modifications to the cold plasma calculations. The major correction and the only necessary one,provided the plasma pressure to the magnetic pressure, β , is small, is the evaluation of the K_{zz} element of the dielectric tensor,where z is the direction of the magnetic field.

Under this assumption any unstable perturbation has to be electrostatic.This is so,since any non-electrostatic disturbance implies a perturbed magnetic field which would produce an increase in the magnetic field energy (a uniform magnetic field has lowest field energy). Since β is low this would more than componsate for any possible decrease in particle energy.

Restrictions for the validity of the scalar dispersion relation are discussed by Baldwin et al (1969).

We further assume that the plasma is infinite,with time invariant electron velocity distribution $f_0(v_\perp, v_\parallel)$ and is immersed in an ambient unperturbed magnetic field.

With these assumptions we now proceed by solving the linearized Vlasov and Poisson's equations. We specialize in one species of particles, namely electrons with charge (-e). The Vlasov equation in vector form,is

$$\frac{\partial f}{\partial t} + \underset{\sim}{v}\cdot\underset{\sim}{\nabla}_x f - \frac{e}{m}\left(\underset{\sim}{E} + \underset{\sim}{v}\wedge\underset{\sim}{B}\right)\cdot\underset{\sim}{\nabla}_v f = 0 \qquad (1.1)$$

and Poisson's equation, is

$$\underset{\sim}{\nabla}\cdot\underset{\sim}{E} = -2\pi n_0 e\int f\, d^3\underset{\sim}{v} \qquad (1.2)$$

where n_0 is the number density.

At equilibrium we have $f = f_0$, $\underline{E} = 0$ and $\underline{B} = \underline{B}_0$. At the perturbed state we have $f = f_0 + f_1$, where f_1 is the lowest order term in the perturbation expansion of the electron velocity distribution and $\underline{E} = \underline{E}_1$.

Since the disturbance is electrostatic, the perturbed electric field, is

$$\underset{\sim}{E}_1 = -\nabla \Phi_1 \qquad (1.3)$$

and assumed to be very nearly parallel to $\underline{k}$. The wave vector Φ_1 is a scalar potential field.

Equation (1.1) requires,

$$\left(\underset{\sim}{v} \wedge \underset{\sim}{B}_0\right) \cdot \frac{\partial f_0}{\partial \underset{\sim}{v}} = 0 \qquad (1.4)$$

f_1 ($\underline{x}$, $\underline{v}$, t) is then determined by the linearized first order equation,

$$\frac{\partial f_1}{\partial t} + \underset{\sim}{v} \cdot \nabla_x f_1 - \left(\frac{e}{m} \underset{\sim}{v} \wedge \underset{\sim}{B}_0\right) \cdot \nabla_{\underset{\sim}{v}} f_1 = \frac{e}{m} \underset{\sim}{E}_1 \cdot \nabla_{\underset{\sim}{v}} f_0 \qquad (1.5)$$

Equation (1.4) requires $f_0 = f_0(v_\perp, v_\parallel)$; where $v_\perp = (v_x^2 + v_y^2)^{\frac{1}{2}}$, $v_\parallel = v_z$, z being the axis parallel to $\underline{B}_0$ and $\underline{v}$ is the electron thermal velocity.

We proceed solving (1.5) by the method of characteristics noting that the left hand side of the equation is the total time derivative, df_1/dt, as we follow the unperturbed trajectory of particles in phase space; i.e. the rate of change of f_1 as "seen" by a particle which at time t is at the phase point ($\underline{x}$, $\underline{v}$), but which is moving through space in the way fixed by the external magnetic field $\underline{B}_0$.

We can therefore write (1.5), as

$$\frac{df_1}{dt} = \frac{e}{m} \underset{\sim}{E}_1 \cdot \underset{\sim}{\nabla}_v f_0 \tag{1.6}$$

The solution of (1.6) is

$$f_1(\underset{\sim}{v}, \underset{\sim}{x}, t) = -\frac{e}{m} \int_{-\infty}^{t} \underset{\sim}{\nabla} \Phi_1(x', t') \cdot \underset{\sim}{\nabla}_v f_0 \, dt' \tag{1.7}$$

Where x',v',t',are the coordinates of a particle which at time t was at x, v.

We have made the lower limit $t = -\infty$ under the assumption that the plasma is undisturbed in the infinite past and the perturbing fields grow from zero.

It is now assumed that f_1 and Φ_1 vary harmonically in space and time as $\exp i(\underline{k}.\underline{x}-\omega t)$ and consequently we have

$$\left.\begin{aligned} f_1 &= \tilde{f} \exp i(\underset{\sim}{k} \cdot \underset{\sim}{x} - \omega t) \\ \Phi_1 &= \tilde{\Phi} \exp i(\underset{\sim}{k} \cdot \underset{\sim}{x} - \omega t) \end{aligned}\right\} \tag{1.8}$$

Substituting from (1.8) for Φ_1 in (1.7) we obtain,

$$f_1 = -\frac{e}{m} \tilde{\Phi} \int_{-\infty}^{t} dt' \exp i \left\{ \underset{\sim}{k} \cdot (\underset{\sim}{x}' - \underset{\sim}{x}) - \omega(t' - t) \right\} i \underset{\sim}{k} \cdot \underset{\sim}{\nabla}_v f_0 \tag{1.9}$$

We can without loss of generality, write $\underline{k} = (k_\perp, 0, k_{\parallel})$. We then obtain from (1.9)

$$f_1 = -\frac{ie}{m} \tilde{\Phi} \int_{-\infty}^{t} dt' \exp i \left\{ \underset{\sim}{k} \cdot (\underset{\sim}{x}' - \underset{\sim}{x}) - \omega(t' - t) \right\} \left\{ \underset{\sim}{k}_\perp \frac{\partial f_0}{\partial v_\perp} + k_\parallel \frac{\partial f_0}{\partial v_\parallel} \right\} \tag{1.10}$$

Where $k_\parallel$ and $k_\perp$ are parallel and perpendicular to B_0 respectively.

Integral (1.10) converges if $\mathcal{I}P(\omega) < 0$. For $\mathcal{I}P(\omega) \geqslant 0$ we must analytically continue.

Let now $\tau = t' - t$. As the components of $\underline{x}(\tau)$ are linear in those of $\underline{v}$ we can write

$$\underset{\sim}{k} \cdot \underset{\sim}{x}(\tau) \equiv \underset{\sim}{v} \cdot \underset{\sim}{p}(\tau) \tag{1.11}$$

Where $\underline{x}(\tau) = \underline{x}' - \underline{x}$ and $\underline{p}(\tau)$ is the same for all particles and is easily calculated. The unperturbed orbit $\underline{x}(\tau)$, with $\Omega = eB_0/m$, the electron gyrofrequency, is easily calculated to be

$$\underset{\sim}{x}(\tau) = \left(\frac{v_x}{\Omega} \sin \Omega\tau + \frac{v_y}{\Omega}\left(1 - \cos \Omega\tau\right),\ \frac{v_x}{\Omega}\left(1 - \cos \Omega\tau\right) + \frac{v_y}{\Omega} \sin \Omega\tau,\ v_z \tau \right) \tag{1.12}$$

From the definition (1.11) we then have

$$\underset{\sim}{p}(\tau) = \left(\frac{k_\perp}{\Omega} \sin \Omega\tau,\ \frac{k_\perp}{\Omega}\left(1 - \cos \Omega\tau\right),\ k_\parallel \tau \right) \tag{1.13}$$

Owing to the axial symmetry with respect to the magnetic field we can write $\underline{v} = (v_\perp \cos\Psi,\ v_\perp \sin\Psi, v_\parallel)$. Therefore from (1.11), (1.12) and (1.13) we have

$$\underset{\sim}{k} \cdot \underset{\sim}{x}(\tau) = \frac{k_\perp v_\perp}{\Omega} \left\{ \sin\left(\Omega\tau + \Psi\right) - \sin\Psi \right\} + k_\parallel v_\parallel \tau \tag{1.14}$$

Using identity $e^{i\gamma\sin\theta} = \sum_{n=-\infty}^{\infty} J_n(\gamma)e^{in\theta}$, where J_n is the Bessel function of the first kind and substituting equation (1.14) in (1.10) we have

$$f_1 = -\frac{ie}{m}\tilde{\Phi}\int_{-\infty}^{0} d\tau\, e^{-i\omega\tau}\sum_{n,m} J_n\left(k_\perp v_\perp/\Omega\right) J_m\left(k_\perp v_\perp/\Omega\right)\exp\Big\{i(n+m)\Psi$$

$$+ in\Omega\tau\Big\}\left\{k_\perp\frac{\partial}{\partial v_\perp}f_0 + k_\parallel\frac{\partial}{\partial v_\parallel}f_0\right\}\frac{1}{2}\Big\{\exp i\left(\Omega\tau+\Psi\right) +$$

$$\exp -i\left(\Omega\tau+\Psi\right)\Big\}e^{ik_\parallel v_\parallel\tau}$$

$$= -\frac{ie}{m}\tilde{\Phi}\int_{-\infty}^{0} d\tau\sum_{n,m} J_n(k_\perp v_\perp/\Omega)J_m(k_\perp v_\perp/\Omega)\exp i(n-m)\Psi\exp -i\tau(\omega-n\Omega)\Big\{k_\perp\frac{\partial f_0}{\partial v_\perp}$$

$$+ k_\parallel\frac{\partial f_0}{\partial v_\parallel}\Big\}\frac{1}{2}\Big\{\exp i\tau\left(\Omega+k_\parallel v_\parallel\right)\exp i\Psi + \exp -i\tau\left(\Omega-k_\parallel v_\parallel\right)\exp -i\Psi\Big\}$$

$$= -\frac{ie}{2m}\tilde{\Phi}\Big[\int_{-\infty}^{0} d\tau\sum_{n,m} J_n\left(k_\perp v_\perp/\Omega\right)J_m\left(k_\perp v_\perp/\Omega\right)\left[k_\perp\frac{\partial f_0}{\partial v_\perp} + k_\parallel\frac{\partial f_0}{\partial v_\parallel}\right]$$

$$\exp i\left(n-m+1\right)\Psi\exp -i\tau\left(\omega-(n-1)\Omega-k_\parallel v_\parallel\right) +$$

$$\int_{-\infty}^{0} d\tau\sum_{n,m} J_n\left(k_\perp v_\perp/\Omega\right) J_m\left(k_\perp v_\perp/\Omega\right)\left\{k_\perp\frac{\partial f_0}{\partial v_\perp} + k_\parallel\frac{\partial f_0}{\partial v_\parallel}\right\}$$

$$\exp i\left(m-n-1\right)\Psi\exp -i\tau\left(\omega-(n+1)\Omega-k_\parallel v_\parallel\right)\Big]$$

Carrying out the time integration and using the identity $\frac{2n}{\gamma}J_n(\gamma) = J_{n-1}(\gamma) + J_{n+1}(\gamma)$ we obtain

$$f_1 = -\frac{e}{m}\tilde{\Phi}\sum_{n,m}\frac{J_n(k_\perp v_\perp/\Omega)J_m(k_\perp v_\perp/\Omega)}{\omega - n\Omega - k_\parallel v_\parallel}\exp i(n-m)\Psi\Big\{k_\parallel\frac{\partial f_0}{\partial v_\parallel}$$

$$+ \frac{n\Omega}{v_\perp}\frac{\partial f_0}{\partial v_\perp}\Big\} \qquad (1.15)$$

The linearized first order Poisson equation is, by using (1.2) and (1.3), given by

$$-\underset{\sim}{\nabla}\cdot\left(\underset{\sim}{\nabla}\Phi_1\right) = -2\pi n_0 e\int f_1 d^3\underset{\sim}{v}$$

or

$$\nabla^2\Phi_1 = -k^2\tilde{\Phi} = -2\pi n_0 e\int f_1 d^3\underset{\sim}{v} \qquad (1.16)$$

Substituting (1.15) in (1.16) and carrying out the Ψ integration we obtain on rewriting

$$1+\frac{\omega_p^2}{k^2}\sum_{n=-\infty}^{\infty}\int d^3\underset{\sim}{v}\,\frac{J_n^2(k_\perp v_\perp/\Omega)}{\omega-n\Omega-k_\parallel v_\parallel}\left\{\frac{n\Omega}{v_\perp}\frac{\partial f_0}{\partial v_\perp}+k_\parallel\frac{\partial f_0}{\partial v_\parallel}\right\}=0 \qquad (1.17)$$

where $\omega_p = (n_0e^2/m)^{\frac{1}{2}}$ is the electron plasma frequency. Equation (1.17) is the scalar dispersion relation and describes the propagation of waves varying as $\exp i(\underline{k}.\underline{x} - \omega t)$ at an arbitrary angle to $\underline{B}_0$.

If we solve (1.17) for $\omega(\underline{k}$ real), exponential growth is implied for $\omega_i < 0$ and decay for $\omega_i > 0$, while $\omega_i = 0$ indicates undamped propagation. Where $\omega = \omega_r + i\omega_i$.

(II. a). CHOICE OF DISTRIBUTION FUNCTION

It has been suggested by Scarf and Fredricks(1973) that the electrostatic waves with frequency spectrum centered about $(3/2)\Omega$, where Ω is the electron gyrofrequency, observed at the night side auroral cusp are correlated with magnetic substorms.

It is useful at this point to give a brief summary of some of the observations and theory that support this view and also to some extent the choice of the hollow distribution function used in this particular problem.

Hones et al (1967) in their initial report of the"thinning" and subsequent thickening of the magnetotail's behaviour during substorms suggested that the thinning of the

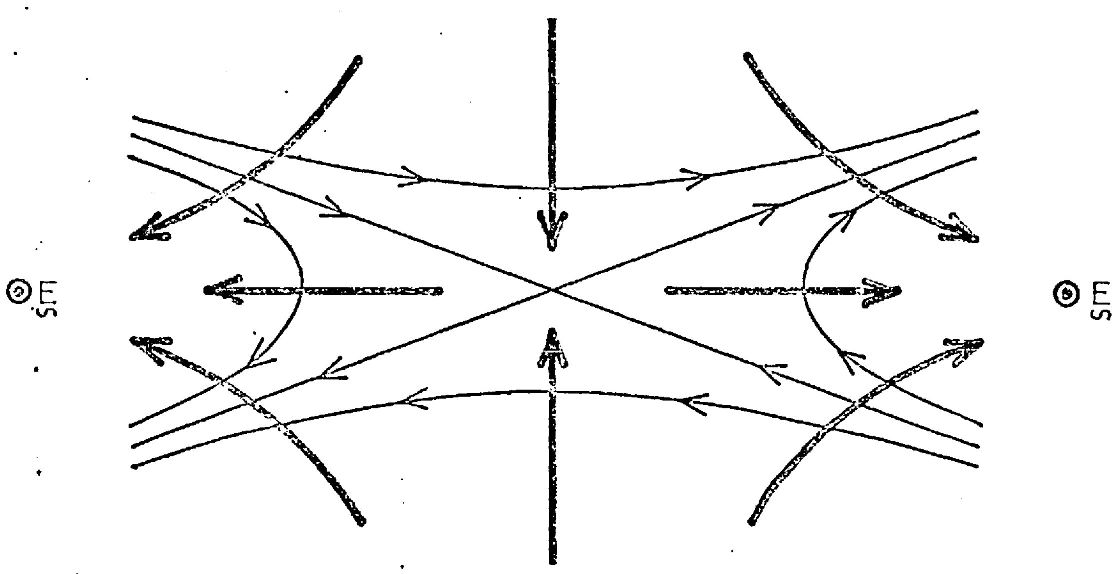

Figure (II·1)

X-type neutral point in the tail formed by the reconnection of field lines during the growth phase of a substorm. Heavy arrows indicate the direction of the magnetic force density.

plasma sheet was caused by displacement of magnetotail plasma towards the earth possibly as a result of merging of the interplanetary and magnetospheric magnetic fields, see figure (II. 1), as suggested by Dungey (1961) and the consequent build up of the tail magnetic field intensity.

A possible accelerating mechanism for these particles would suggest a loss-cone type distribution. If a particle moving in the direction in which it is accelerated deviates in a direction perpendicular to the magnetic field, the magnetic field brings it back so that it stays in the region of high current density. If it deviates in a direction along the magnetic field, the magnetic field bends its orbit further away so that the orbits fan out in this direction. The fanning out may reduce their density below that of the back-ground plasma which can then neutralize the space charge.

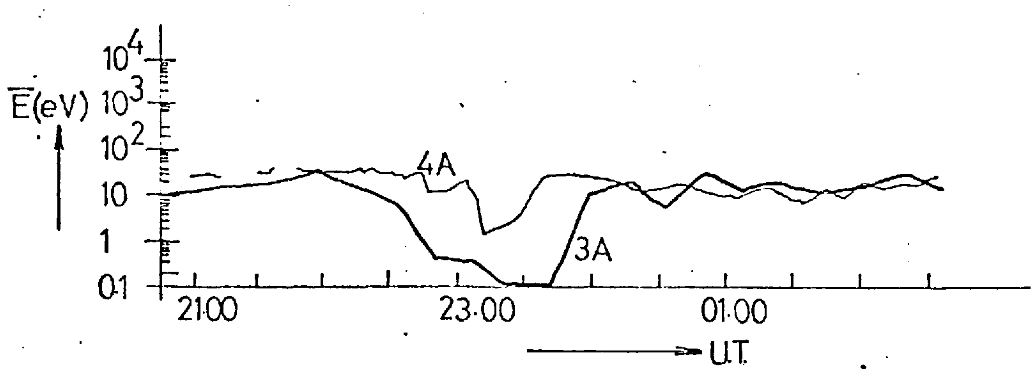

Figure (II-1a)

Data from Vela 3A and 4A showing the average electron energy, $\overline{E}$, at $R \simeq 18$. (After Hones, 1971)

Scarf and Fredricks(1971) reported from OGO 5 data obtained at the location $7.6 \leqslant L \leqslant 7.9$, LT. 00.45 and $1.9^{\circ} \leqslant$ MLAT $\leqslant 2.9^{\circ}$, that a few minutes (~ 4) after the onset of a substorm expansion, when the field first settled to a dipolar configuration, a loss-cone distribution of electrons with $E \simeq 80$ keV was detected. Soon after however the distribution became quite isotropic and very intense $\omega \simeq (3/2)\Omega$ waves accompanied the particle isotropy. These waves have generally been observed between $4 \leqslant L \leqslant 10$ in the midnight-down-noon local time sector.

An electron energy distribution observed by Vela 3A and 4A satelites during the thinning process of the plasma sheet, discussed in detail by Hones et al (1971b) is shown in figure (II.1a). This observation seems to be consistent with the idea that energetic electrons injected from the plasma sheet into the midnight region during substorms are convected inwards and subsequently energized. Similar observational evidence is supported by Lezniak and Winkler (1970) and DeForest and McIlwain (1971), the latter workers used measurements in the region $L \simeq 6.6$. A distribution of the location where intense flux of electrons of $E > 10$ keV is observed, is shown in figure (II. 1b) and a graph of the energy density of electrons as a function of L, in the range $2 \leqslant L \leqslant 8$ is shown in figure (II. 1c). The orbit of OGO 3 is also shown so that the energy density distribution with respect to L.T. can be estimated. For the choice of the particular distribution function of figure (II. 2) it was assumed that particles with high energies are distributed a-

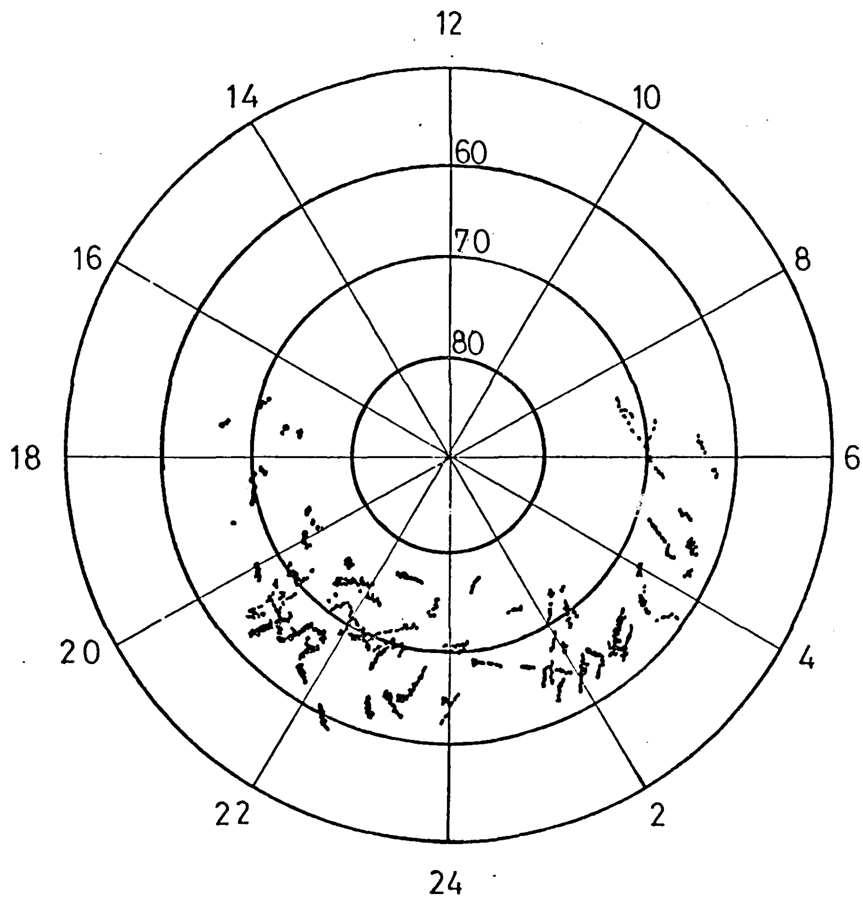

Figure (II·1b)

Distribution of the locations where intense flux of electrons of $E > 10$ KeV was observed. (After Fritz and Gurnett, 1965) long the 24.00 L.T. sector with a sharp drop in energy at L.T. away from midnight but with energy remaining greater than zero.

Now to allow for the loss-cone we take $S(v_\perp)$ distribution such that

$$S(v_\perp) = \begin{cases} 0 & \text{for} \quad v_\perp < V_o \\ 1 & \text{for} \quad v_\perp \geqslant V_o \end{cases}$$

This is equivalent to a pitch angle distribution modified so as to retain more particles with highest $v_\perp$ and lowest $v_\parallel$, which would otherwise fall within the loss-cone α_1, refer to figure (II. 2) . Further, the particles are allowed

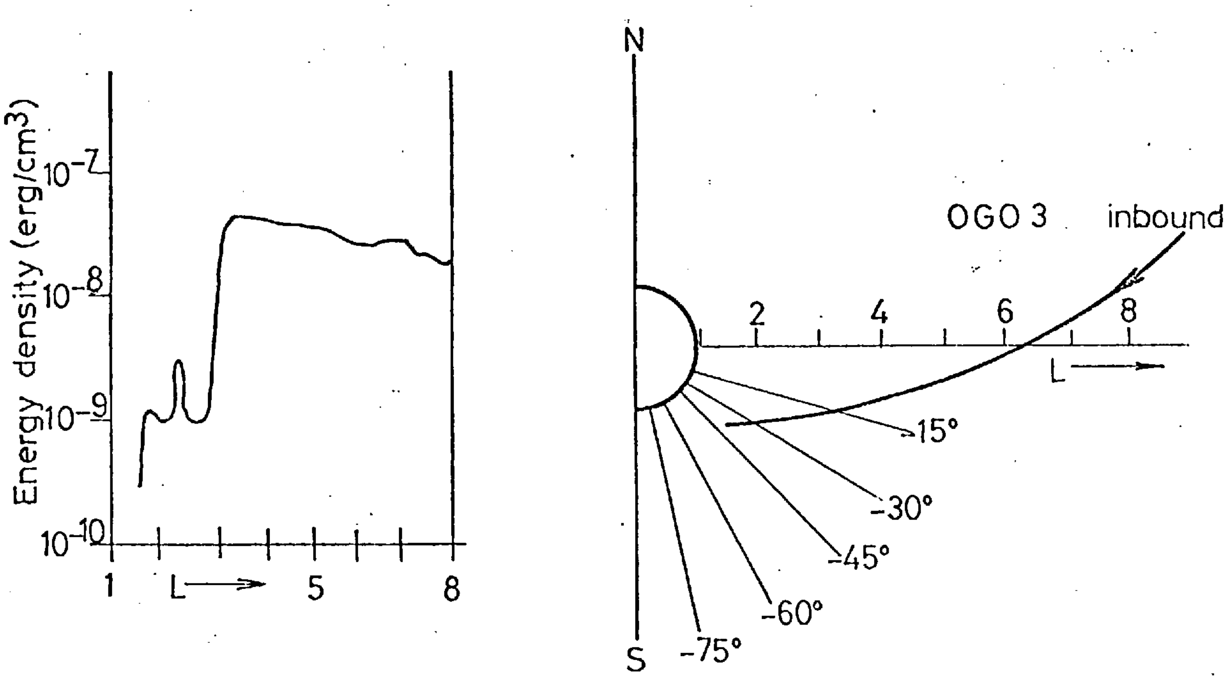

Figure(II.1c)

Electron $200 \leqslant E \leqslant 50{,}000$ eV energy densities as function of L during the main phase of the early July 1966 storm some spread in their velocity distribution $g(\underline{v} - \underline{V})$ which is peaked away from $\underline{v} = 0$.

With

$$g(\underset{\sim}{v} - \underset{\sim}{V}) = \begin{cases} 0 \text{ for } & \underset{\sim}{v} \geqslant V_2 \text{ and } \underset{\sim}{v} \leqslant V_1 \\ \dfrac{3}{4\pi(V_2 - V_1)^3} & \text{for } V_1 \leqslant \underset{\sim}{v} \leqslant V_2 \end{cases}$$

representing in velocity space a spherical shell of normalized density.

We now take a zero order distribution function

$$f_0 = g(\underset{\sim}{v} - \underset{\sim}{V})\, S(v_\perp)$$

represented in $v_\perp$, $v_\parallel$ plane by a circular anulus.

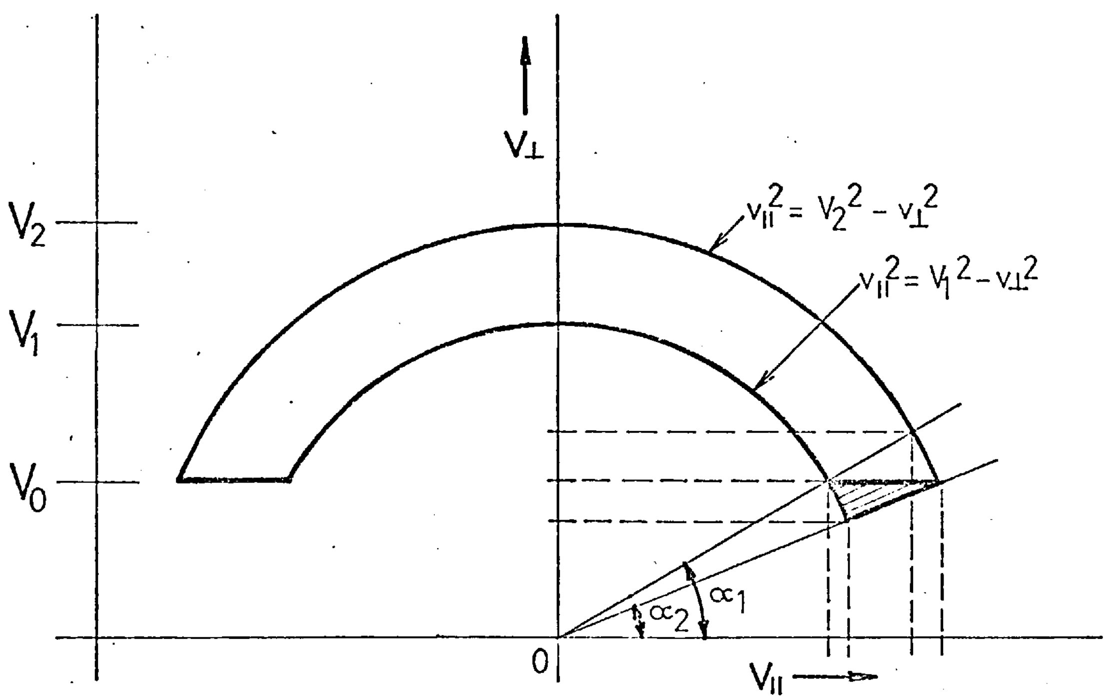

Figure (II·2)
The distribution function $f_0 = g(\underline{v} - \underline{V})S(v_\perp)$

(II.b) Dispersion relation for perpendicular propagation

If we now specialize (I.17) for perpendicular propagation only, i.e. $k_\parallel = 0$, we obtain

$$\mathcal{D}(\omega,k_\perp) \equiv 1 + \frac{\omega_p^2}{k_\perp^2}\sum_{n=-\infty}^{\infty}\int d^3\underline{v}\left(\frac{n\Omega}{\omega - n\Omega}\right)\frac{1}{v_\perp} J_n^2\left(k_\perp v_\perp/\Omega\right)\frac{\partial f_0}{\partial v_\perp} \qquad (\text{II}.1).$$

Taking cylindrical polar coordinates (II.1) becomes

$$\mathcal{D}(\omega,k_\perp) \equiv 1 + \frac{\omega_p^2}{k_\perp^2}\sum_{n=-\infty}^{\infty}\int_{v_\perp}\int_{v_\parallel}\int_0^{2\pi}\frac{n\Omega}{\omega - n\Omega} J_n^2\left(k_\perp v_\perp/\Omega\right)\frac{\partial}{\partial v_\perp} f_0\, dv_\perp dv_\parallel d\Phi \qquad (\text{II}.2).$$

Adding the contributions of the annulus f_0, figure (II.2) and performing the Φ integration (II.2) gives

$$\mathcal{D}(\omega,k_\perp) \equiv 1 + \frac{2\pi\omega_p^2}{k_\perp^2}\sum_{n=-\infty}^{\infty}\frac{n\Omega}{\omega - n\Omega}\Bigg[\int_{V_1}^{V_2}\left\{J_n^2\left(k_\perp v_\perp/\Omega\right)\frac{3}{4\pi(V_2-V_1)^3}\frac{\partial}{\partial v_\perp}\int_0^{(V_2^2-v_\perp^2)^{1/2}} dv_\parallel\right\}dv_\perp +$$

$$\int_{V_0}^{V_1}\left\{J_n^2\left(k_\perp v_\perp/\Omega\right)\frac{3}{4\pi(V_2-V_1)^3}\frac{\partial}{\partial v_\perp}\int_{(V_1^2-v_\perp^2)^{1/2}}^{(V_2^2-v_\perp^2)^{1/2}} dv_\parallel\right\}dv_\perp\Bigg] \qquad (\text{II}.3).$$

In (II.3) $\frac{\partial}{\partial v_\perp}$ was taken outside the integral of $v_\parallel$, since $v_\parallel$ and $v_\perp$ are independent variables. Performing the $v_\parallel$ integration followed by an integration by parts, we obtain on rearranging

$$\mathcal{D}(\omega,k_\perp) \equiv 1 - \frac{2\pi\omega_p^2}{k_\perp^2}\frac{3}{4\pi(V_2-V_1)^3}\sum_{n=-\infty}^{\infty}\frac{n\Omega}{\omega-n\Omega}\Bigg[J_n^2\left(k_\perp V_0/\Omega\right)\Big[(V_2^2-V_0^2)^{1/2} -$$

$$(V_1^2-V_0^2)^{1/2}\Big] + \int_{V_1}^{V_2}\frac{\partial}{\partial v_\perp}J_n^2\left(k_\perp v_\perp/\Omega\right)(V_2^2-v_\perp^2)^{1/2}\,dv_\perp + \int_{V_0}^{V_1}\frac{\partial}{\partial v_\perp}J_n^2\left(k_\perp v_\perp/\Omega\right)$$

$$\left(V_2^2-v_\perp^2\right)^{1/2} dv_\perp - \int_{V_0}^{V_1} \frac{\partial}{\partial v_\perp} J_n^2\left(k_\perp v_\perp/\Omega\right)\left(V_1^2-v_\perp^2\right)^{1/2} dv_\perp \Bigg] \qquad (\mathrm{II}.4)$$

Let,

$$\begin{aligned} k_\perp v_\perp/\Omega &= z \\ k_\perp V_\perp/\Omega &= z_0 \\ \text{and} \quad \frac{\partial z}{\partial v_\perp} &= k_\perp/\Omega = \beta \end{aligned} \qquad (\mathrm{II}.5)$$

Substituting for (II.5) in (II.4) and normalizing the limits of integration, we obtain

$$\mathscr{D}(\omega,k_\perp) \equiv 1 - \frac{2\pi\omega_p^2}{k_\perp^2}\,\frac{3}{4\pi\left(V_2-V_1\right)^3}\sum_{n=0}^{\infty}\frac{n\Omega}{\omega-n\Omega}\Bigg\{\Bigg[\left(V_2^2-V_0^2\right)^{1/2}-\left(V_1^2-V_0^2\right)^{1/2}\Bigg]J_n^2(z_0) + \int_{\beta V_1}^{\beta V_2}\frac{\partial}{\partial z}\left[J_n^2(z)\right]\left(V_2^2-z^2/\beta^2\right)^{1/2}dz + \int_{\beta V_0}^{\beta V_1}\frac{\partial}{\partial z}\left[J_n^2(z)\right]\left(V_2^2-z^2/\beta^2\right)^{1/2}dz - \int_{\beta V_0}^{\beta V_1}\frac{\partial}{\partial z}\left[J_n^2(z)\right]\left(V_1^2-z^2/\beta^2\right)dz\Bigg\} \qquad (\mathrm{II}.6)$$

By using Bessel function recurrence relations (II.7)

$$\begin{aligned} 2J_n'(z) &= J_{n-1}(z) - J_{n+1}(z) \\ \frac{2n}{z}J_n(z) &= J_{n-1}(z) + J_{n+1}(z) \end{aligned} \qquad (\mathrm{II}.7)$$

with primed quantities denoting derivatives with respect to z and noting that (II.6) is identically zero for n=0 we obtain on rewriting

$$\mathscr{D}(\omega,k_\perp)\equiv 1-\frac{2\pi\omega_p^2}{k_\perp^2}\,\frac{3}{4\pi\left(V_2-V_1\right)^3}\,\frac{1}{\beta}\sum_{n=1}^{\infty}\frac{\Omega}{\omega-n\Omega}\left\{n\left[\left(\beta^2V_2^2-\beta^2V_0^2\right)^{1/2}-\right.\right.$$

$$\left.\left(\beta^2V_1^2-\beta^2V_0^2\right)^{1/2}\right]J_n^2(z_0)+\frac{1}{2}\left[\int_{\beta V_1}^{\beta V_2}\left(J_{n-1}^2(z)-J_{n+1}^2(z)\right)\left(\beta^2V_2^2-z^2\right)^{1/2}z\,dz+\right.$$

$$\left.\left.\int_{\beta V_0}^{\beta V_1}\left(J_{n-1}^2(z)-J_{n+1}^2(z)\right)\left[\left(\beta^2V_2^2-z^2\right)^{1/2}-\left(\beta^2V_1^2-z^2\right)^{1/2}\right]z\,dz\right]\right\} \qquad (\text{II}.8)$$

The dispersion relation for perpendicular propagation is simply (II.8) set equal to zero,

$$\mathscr{D}\left(\omega,k_\perp\right)=0 \qquad (\text{II}.9)$$

It is evident that there is no possible analytical solution for (II.9). A numerical solution was therefore sought to establish the conditions for instability and investigate its dependence on the parameters of the velocity distribution function.

(III). FORMULATION OF THE COMPUTATIONAL PROBLEM AND METHOD OF INVESTIGATION

In order to investigate how the parameters of the distribution function and the argument of the Bessel functions, z_0, determine the onset of instability, solutions of the dispersion relation were computed for a range of values of the velocity spread to pitch angle ratio,

$$\frac{V_2-V_1}{V_0} \equiv x_0 = 0{\cdot}5\,,\ 1\,,\ 2 \qquad \text{(III.1)}$$

and maximum perpendicular velocity to pitch-angle ratio,

$$\frac{V_2}{V_0} = 3\,,\ 5\,,\ 7,\ 10\,,\ 100 \qquad \text{(III.2)}$$

for

$$0{\cdot}2 \leqslant z_0 \equiv \frac{k_\perp V_0}{\Omega} \leqslant 3 \qquad \text{(III.3)}$$

For values of z_0 between 0 and 0.2 the investigation carried out was analytic. See appendix I.

To discuss the various solutions possible it is useful to rewrite the dispersion relation (II.8) in the form,

$$\mathcal{D}(\omega,k_\perp) \equiv 1 - \frac{2\pi\omega_p^2}{K_\perp^2}\,\frac{3}{4\pi}\,\frac{1}{(V_2-V_1)^3}\,\frac{1}{\beta}\,F(W) \qquad \text{(III.4)}$$

with,

$$F(w) \equiv \sum_{n=1}^{10} \left(\frac{1}{w-n}\right) I_n \qquad (\text{III}.5)$$

Where I_n are the Bessel function coefficients and

$$w = \frac{\omega}{\Omega} \qquad (\text{III}.6)$$

Rewriting (III . 4) we obtain,

$$F(w) = \frac{2}{3}\frac{k_\perp^2(V_2-V_1)^3}{\omega_p^2}\beta \qquad (\text{III}.7)$$

Substituting (II .5) and (II. 2) in the above equation the dispersion relation can be written as,

$$F(w) = \frac{2}{3}\left(\frac{\Omega}{\omega_p}\right)^2 x_0^3 z_0^3 \qquad (\text{III}.8)$$

This yields four different types of solution, illustrated in figure (III . 1).

If F(w) is plotted versus w, the roots of the dispersion relation are the intersections of the curve, F(w) versus w, with the horizontal line

$$f(w) = \frac{2}{3}\left(\frac{\Omega}{\omega_p}\right)^2 x_0^3 z_0^3 .$$

Where f(w) represents any point on the F(w) axis such that $0 \leqslant f(w)$.

The condition for instability is the loss of real roots, i.e. that the horizontal line $3/2(\Omega/\omega_p)^2 x_0^3 z_0^3$ does not intersect the curve for real positive values of $(\Omega/\omega_p)^2$.

Referring to figure (III . 1), we can see that in the case of curve type I and for any value of the line $3/2(\Omega/\omega_p)^2 x_0^3 z_0^3$ less than a critical value , given by the minimum point of F(w) curve, there is no real root solution.

From this minimum value of the line,

$$F(W)_{min} = \frac{2}{3}\left(\frac{\Omega}{\omega_p}\right)^2 \left(x_0 z_0\right)^3 \qquad \text{(III. 9)}$$

we can obtain the minimum plasma density for critical stability, for a given distribution function, z_0 and Ω .

As it was mentioned in the introduction, solutions for the high frequency regime Bernstein modes exist only for $F(w) > 0$ i.e.in the high frequency side of the asymptotes

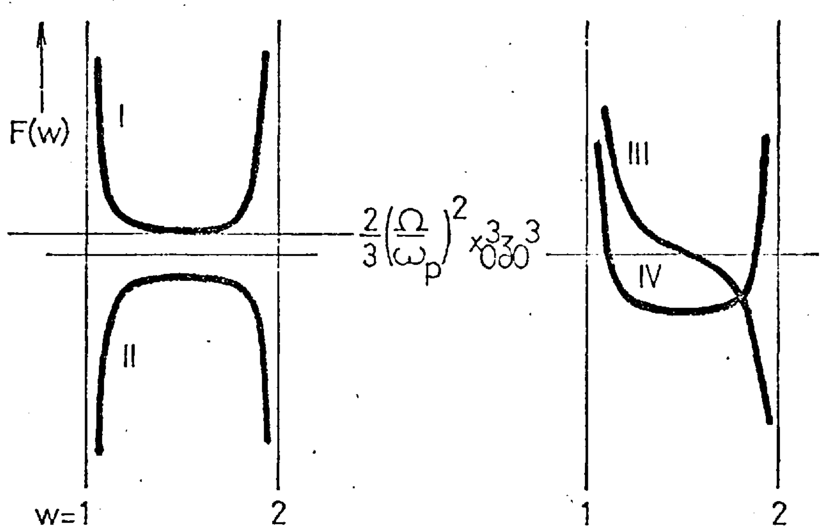

Figure (III ·1)
Solutions of the dispersion relation for the same distribution function and four different values of z_0

$\omega = n\Omega$. Curve II, therefore, does not represent a solution for the $(n + \frac{1}{2})\Omega$-waves and need not concern us any further. There is a last point to be mentioned and this is that this curve might, however, represent lower frequency instabilities and since it appears in the numerical solutions, it shall be referred to as the case of "possibly unstable" modes.

In case IV there exist only stable mode solutions for any real value of ω_p.

The necessary and sufficient condition to obtain any of the above three types of curve is that $I_1 I_2 < 0$, where I_1 and I_2 refer to the Bessel function coefficients with $n = 1$ and $n = 2$.

If coefficients I_1 and I_2 have the same sign, i.e. $I_1 I_2 > 0$, curves of the type III are only possible and consequently there are only stable mode solutions.

Although a comparison of I_1 and I_2 coefficients is not sufficient to determine whether instability is possible, it can however indicate the regions of z_0 where stability is only possible. This method was used to investigate the behaviour of $F(w)$ as z_0 approaches zero,(appendix I).

Some graphs of the function $F(w)$ plotted against w, for different values of z_0 are shown in figures (III . 2a) and (III . 2b).

The necessary and sufficient condition for instability is

$$I_1 I_2 < 0 \quad \text{and} \quad F(w) > 0 \quad \text{for all } w \qquad (\text{III} . 10)$$

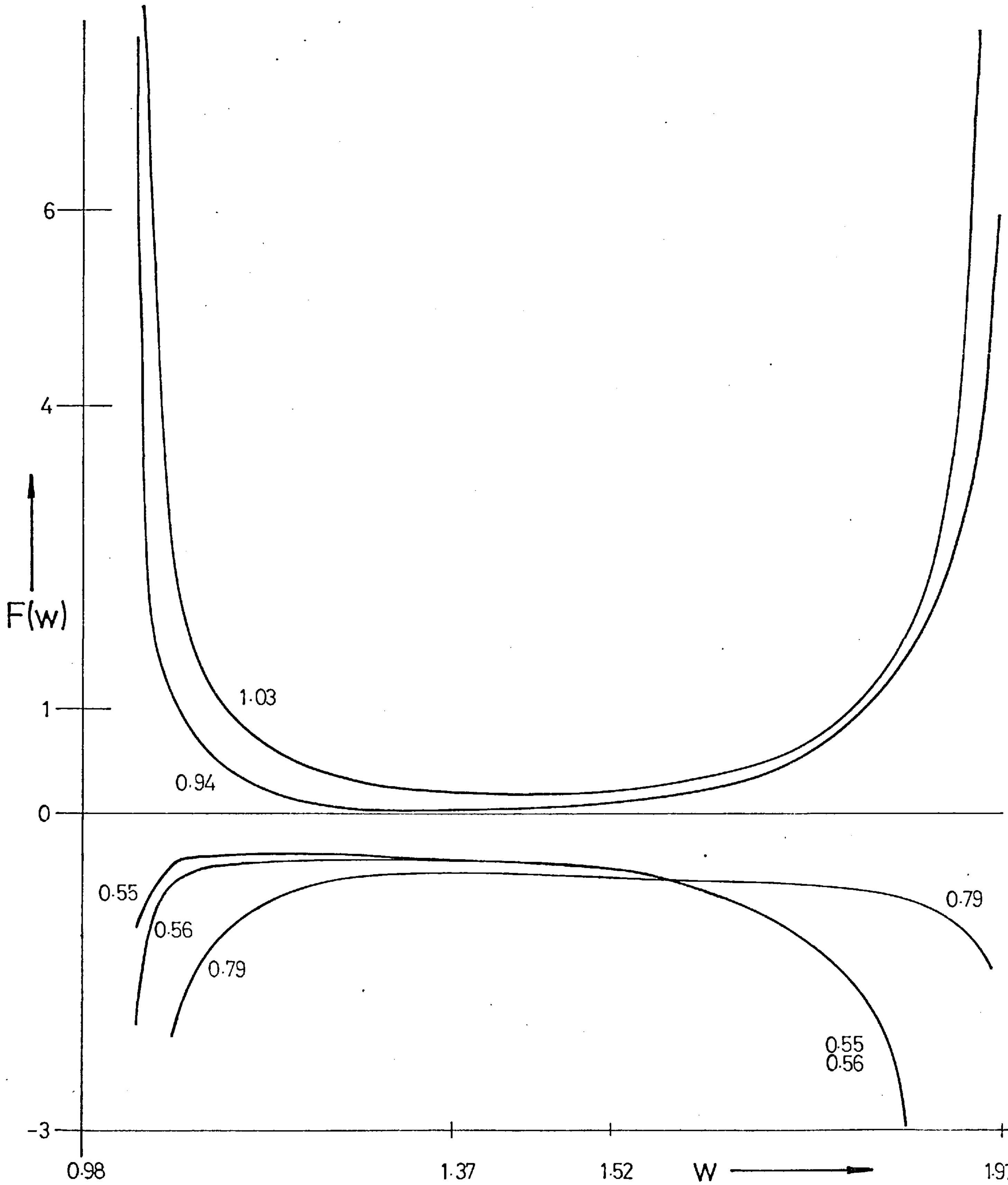

Figure (III · 2a)

Plot of F(w) versus w illustrating solutions of the dispersion relation (III · 4) for different values of z_0, giving critically stable and possibly unstable solutions.

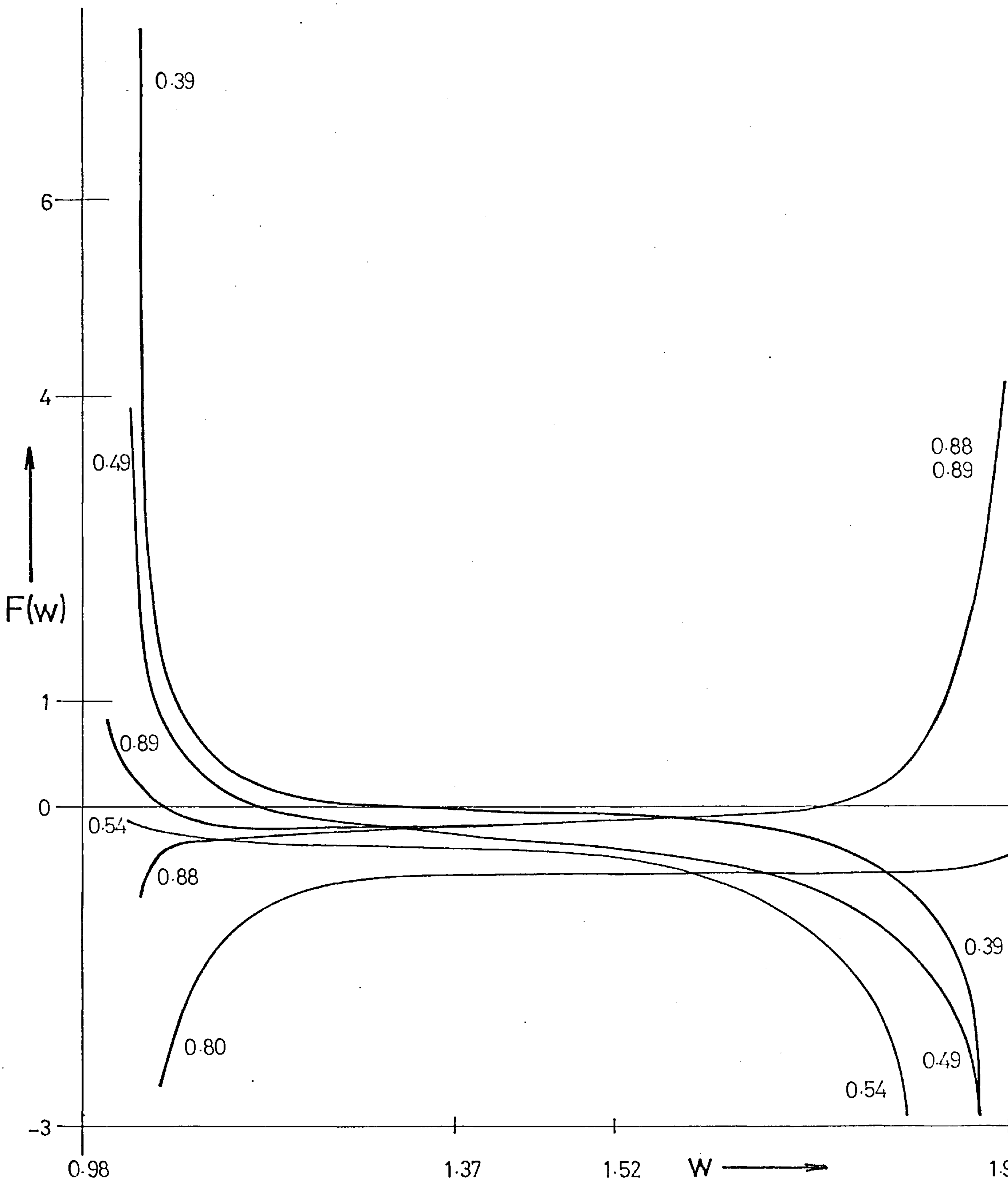

Figure (III·2b)

Plot of F(w) versus w illustrating solutions of the dispersion relation (III·4) for different values of z_0, giving stable solutions only

Condition (III . 10) being satisfied, there is a minimum value of the plasma density for which unstable mode solutions are possible, which means that instability is bound in each case by minimum plasma frequency.

For a given distribution function it is the value of z_0 that determines the type of solution possible for any branch of the curve F(w) versus w.

The behaviour of the function F(w) for the branch lying between $1 \leqslant w \leqslant 2$ and for increasing z_0, is illustrated qualitatively in figure (III . 5).

Curves for F(w) versus w for increasing values of w are shown in figure (III . 3) and figure (III . 4). The figures

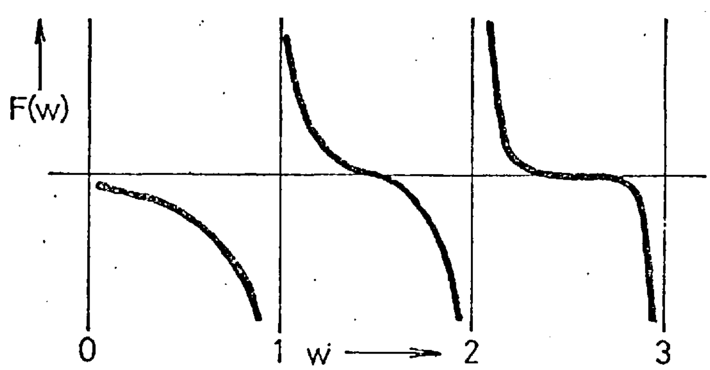

Figure (III·3)

Plot of F(w) versus w for a given distribution function and given z_0 giving stable solutions

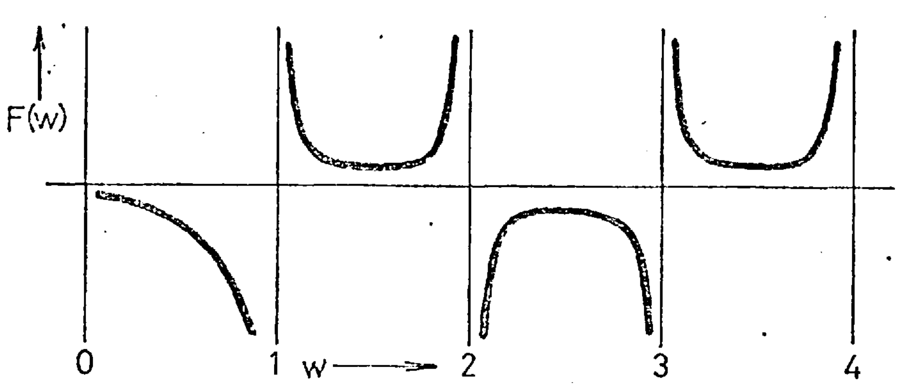

Figure (III·4)

Plot of F(w) versus w for the same distribution function but different z_0 giving unstable solutions

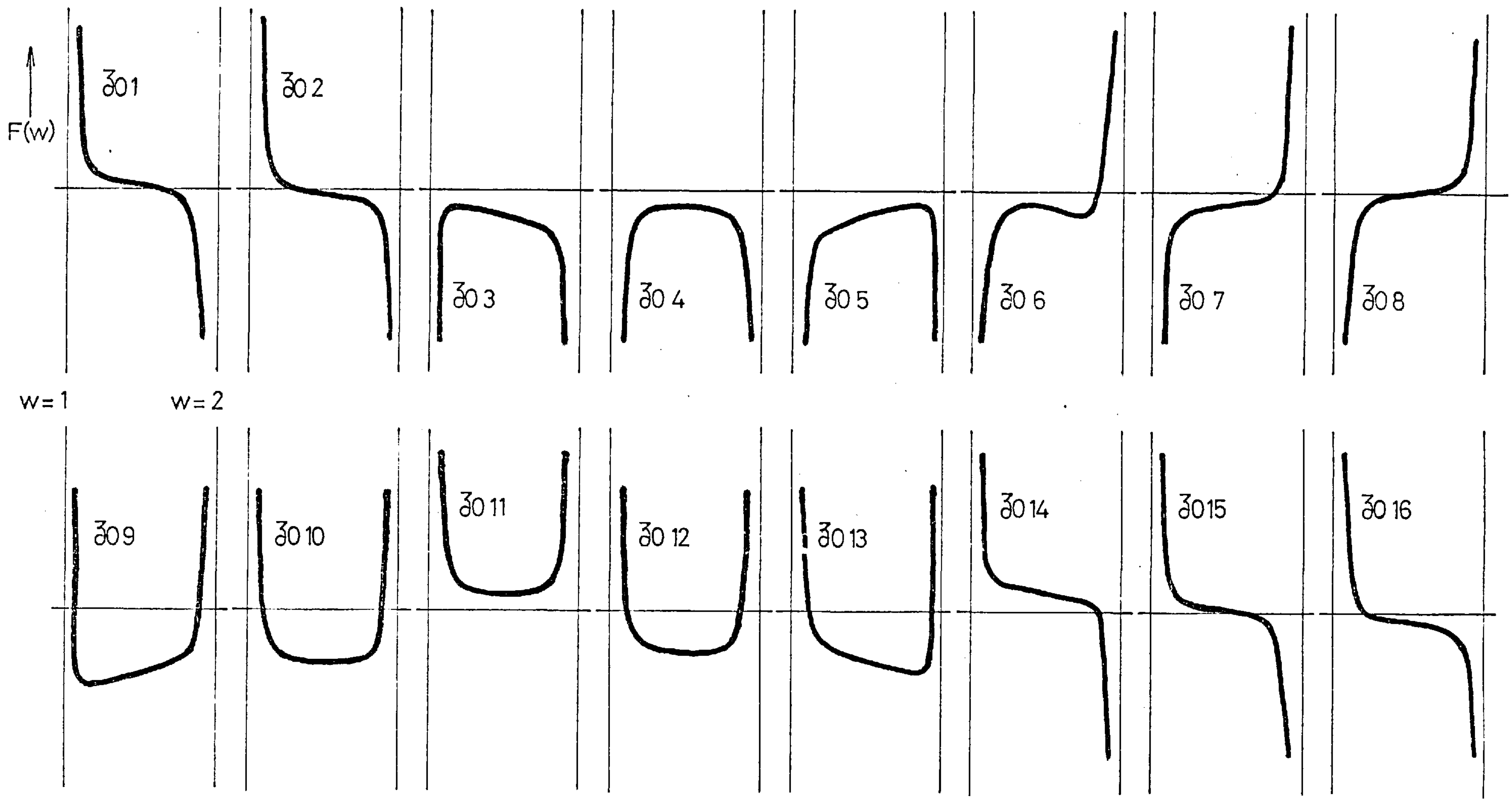

Figure (III·5)

Typical behavior of the function $F(w)$ for a given distribution function and for $1 \leqslant w \leqslant 2$ as z_0 increases are plotted for two different values of z_0 giving stable and unstable mode solutions respectively.

In order to compute F(w) the first step was to evaluate the Bessel functions for a given argument and integer order.

For this the recurrance relation

$$J_{n+1}(z) + J_{n-1}(z) = \frac{2n}{z} J_n(z)$$

was used, the desired Bessel function being

$$\mathcal{J}_n(z) = J_n(z)/\alpha$$

where

$$\alpha = J_0(z) + 2\sum_{m=1}^{M-2} J_{2m}(z)$$

This method imposes the limitation that

$$M_{max.} = N = \begin{cases} (20+10z-z^2/3) & \text{for } z \leqslant 15 \\ (90+z/2) & \text{for } z > 15 \end{cases}$$

The series of the Bessel functions was truncated at N=10, see equation (III . 5), as it is very rapidly convergent and contributions of the terms with n > 10 were found to be negligible within the required accuracy for the remaining computation of the problem.

For the evaluation of the integrals the Modified Romberg Algorithm was used with cosine transforms. The function F(w) was then computed for a range of values of z_0 and for different distribution functions. See equations (III . 1), (III . 2) and (III . 3).

As mentioned before, for a given z_0 , critical stability can occur and in order to obtain the value of plasma density for which this is possible, it is necessary to compute the exact minimum of the curve and the corresponding values of w and z_0 for which it occurs.

To do this the function F(w) was optimized with respect to $w \geqslant 0$.

To minimize F(w) a polynomial fitting was used and by gradient and function evaluations the interval of uncertainty within which the minimum of F(w) lies was reduced. The optimization problem was solved when the length of the interval of uncertainty was sufficiently small.

In the use of the above method the following two assumptions about the behaviour of F(w) are implicit. One that the function is sufficiently smooth for a low order polynomial (cubic in this case) to be a good approximation to it and two, that the function is differentially unimodal on the interval of uncertainty, i.e. it has a proper global minimum on this interval and no other local minima and its derivative F'(w) satisfies

$$F'(w) > 0 \quad \text{for} \quad w_{min.} < w$$
$$F'(w) < 0 \quad \text{for} \quad w_{min.} > w \, .$$

(IV). FACTORS AFFECTING INSTABILITY

From the computational analysis it was established that the factors influencing instability are, the argument of the Bessel functions, z_0, the relative spread of the perpendicular velocities of the distribution function and maximum to minimum perpendicular velocity ratio.

Although all three factors operate simultaneously to produce instability, it is useful to look at them separetely and establish how instability depends on each one of them.

The first point to discuss is the dependence of the instability on the value of z_0. As we shall see, the minimum value of the critical plasma density for instability occurs at a given value of z_0. This critical value of z_0 would give the most unstable $k_\perp$.

For this analysis a particular distribution function was chosen, one with

$$\frac{V_2-V_1}{V_0} = 0.5 \qquad \text{and} \qquad \frac{V_2}{V_0} = 5$$

and the behaviour of the function F(w) was computed for increasing values of z_0 and for $1 \leqslant w \leqslant 2$.

It was found that as z_0 increases gradually from zero to $z_0 = 0.55$ only stable modes are possible. Their solutions, represented qualitatively in figure (III . 5) by curves of the type z_{01} and z_{02}, form the first stable "band" in z_0, illustrated in figure (IV. 6).

As z_0 increases from zero curves progress from type z_{01} to z_{02}. At $z_0 = 0.56$ the curves change abruptly to type z_{03},

z_{04}, z_{05}, gradually again progressing from z_{03} to z_{05} and form the "possibly unstable band" , of figure (IV. 6) between $0.56 \leqslant z_0 \leqslant 0.79$. Curves z_{06}, z_{07}, z_{08} and z_{09} correspond to the second stable band, $0.80 \leqslant z_0 \leqslant 0.93$ and curve z_{011} corresponds to the first "critically" stable band between $0.94 \leqslant z_0 \leqslant 1.13$.

The term "critically stable band" is employed to indicate that instability is only possible if $(\Omega/\omega_p)^2$ is greater than a minimum value, given by the minimum point of the F(w) curve. This minimum point will in future be referred to as the "critical plasma density", since for a given Ω, ω_p can be calculated and hence the density of the plasma for critical stability.

From z_{012} to z_{014}, the next stable band starts forming progressing to z_{015} which qualitatively corresponds to z_{01} and there on the behaviour repeats for increasing values of z_0.

However as z_0 increases and curves repeat in shape, two major differences occur. One, that the width of the bands alters and the other, that the extremum of the curves approaches a limiting value.

It is of interest to elaborate further on this point. As z_0 increases,

$$1.5(F(w)_{min.}/x_0^3\ z_0^3) \equiv (\frac{\Omega}{\omega_p})^2 ,$$

which gives the value of the critical plasma density, tends

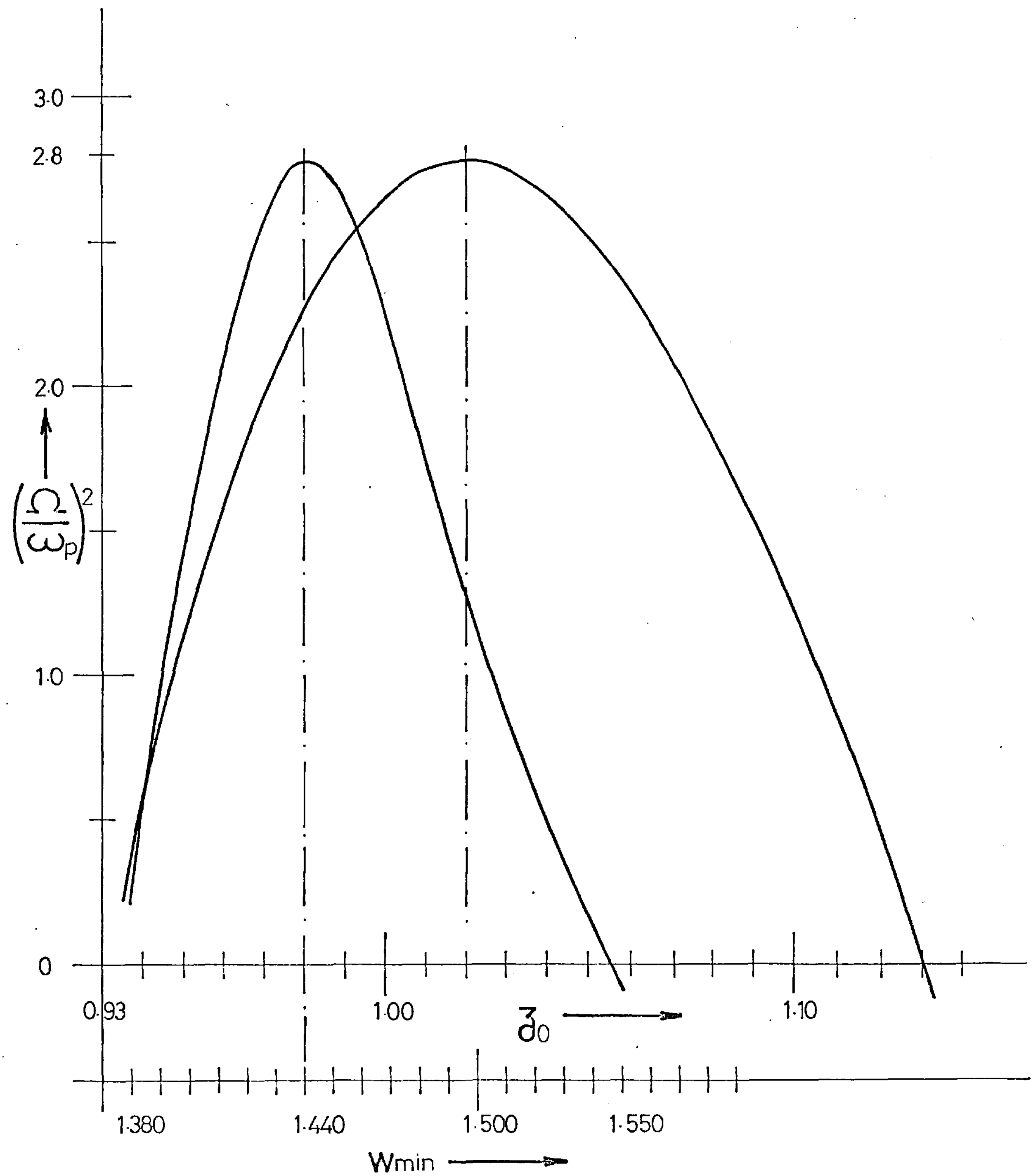

Figure (IV·1)

Plot of $1.5\,(F(w)_{min}/x_0^3\,\mathfrak{z}_0^3) \equiv (\Omega/\omega_p)^2$ versus w min and $\mathfrak{z}_0$ for the first unstable band of the distribution function $V_2-V_1/V_0 = 0.5$ and $V_2/V_0 = 5$ showing the variation of the critical plasma density with $\mathfrak{z}_0$ and w min

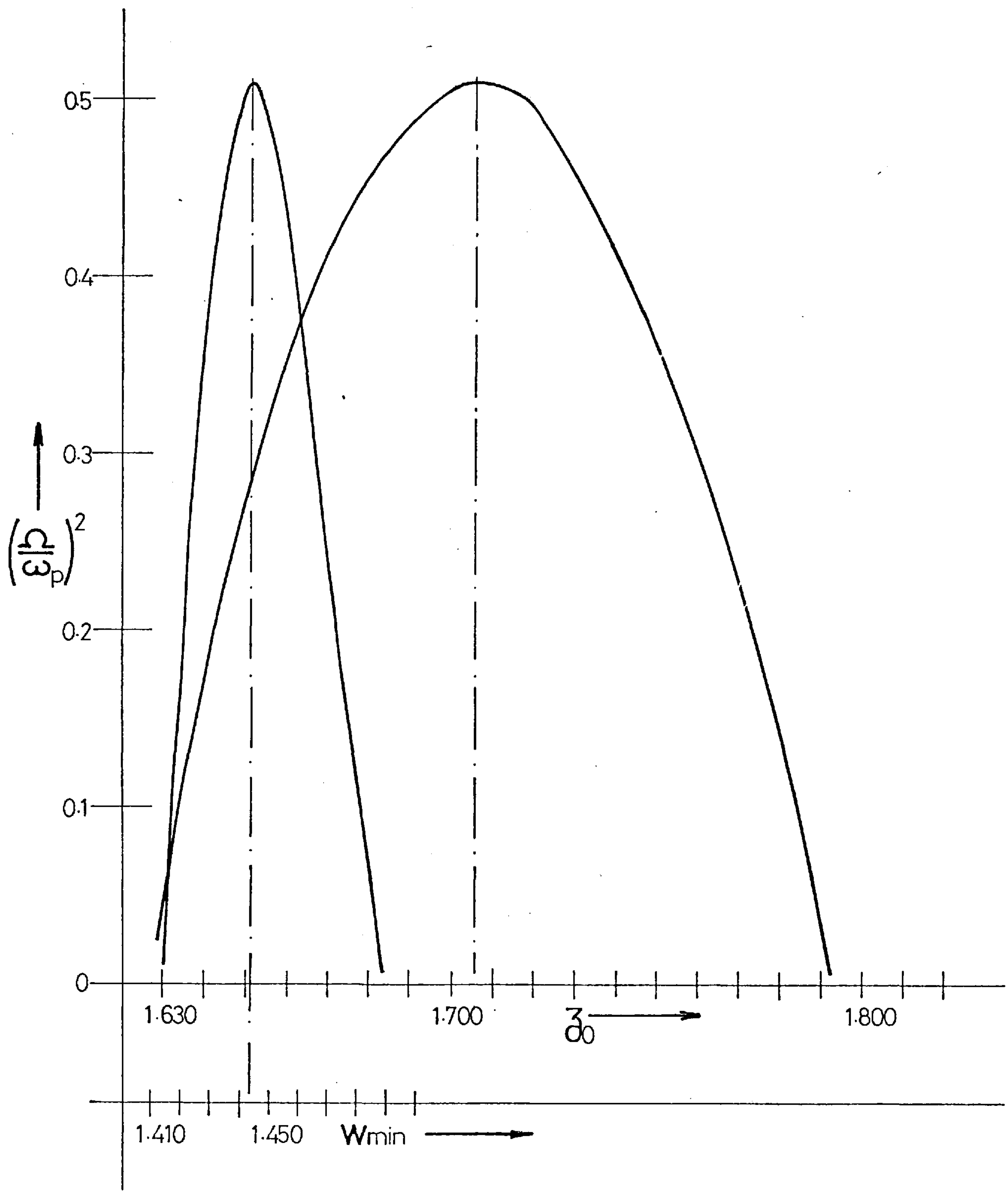

Figure (IV·2)

Plot of $(\Omega/\omega_p)^2$ versus w min and z_0 for second unstable band of the distribution function $V_2-V_1/V_0=0.5$ and $V_2/V_0=5$

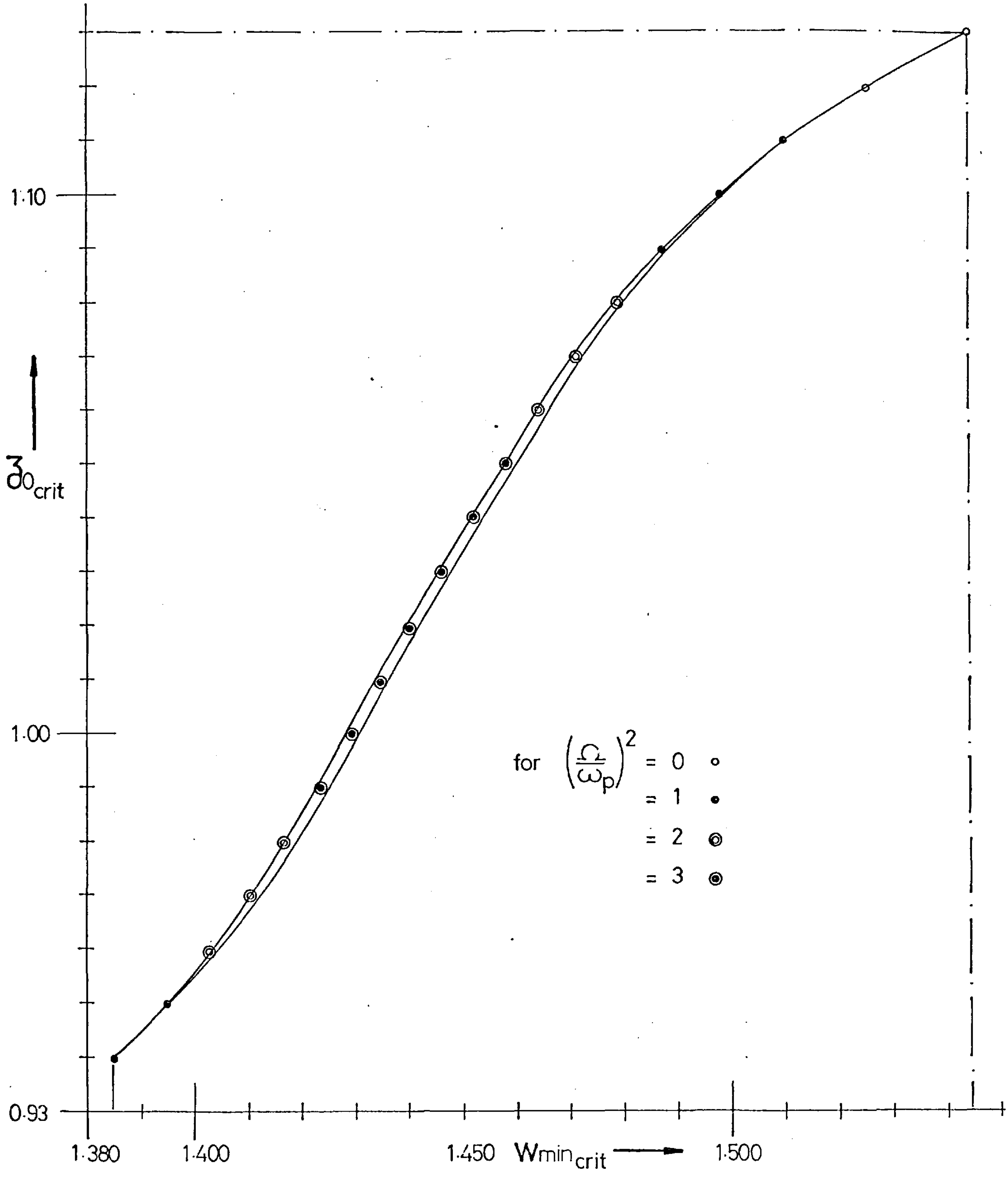

Figure (IV·3)

Plot of the surface of constant $(\Omega/\omega_p)^2$ for the first critically stable band of the distribution function $(V_2-V_1)/V_0 = 0{\cdot}5$ and $V_2/V_0 = 5$

to zero. That means that instability is only possible for infinite plasma density and consequently the plasma is always stable.

It is worth noting that $(\Omega/\omega_p)^2$ tends to zero very fast with increasing z_0. Compare figures (IV. 1) and (IV. 2). Plasma density therefore becomes infinite for moderately short wavelengths. For wavelengths shorter than a critical value the plasma is always stable. The minimum wavelength for which unstable mode solutions exist is dependent on the parameters of the distribution function. This will be discussed further, later on in this chapter.

Figures (IV. 1) and (IV. 2) illustrate the relative decrement in band widths of z_0 and $w_{min.}$, for increasing values of z_0. They also indicate the value of minimum critical plasma density for the first and second unstable bands and the corresponding value of z_0 and $w_{min.}$ at minimum critical plasma density.

Now, for instability in general, the values of w lie between $1.35 \leqslant w \leqslant 1.65$ but $w_{min.}$ never exceeds the range $1.4 \leqslant w_{min.} \leqslant 1.5$ for any value of the distribution function. See table (IV. 1).

A typical contour of critical plasma density is plotted in figure (IV. 3). It can be seen that unstable solutions are bound by an upper and lower value in z_0. The minimum value of z_0 would give the first unstable $k_\perp$.

As the stable Bernstein modes, therefore, unstable modes are also bound by a maximum and minimum frequency but in contrast to them solutions only exist for a given range of the wavelength. This range as it will be seen later on, diminishes with decreasing wavelength. Eventually solutions become only possible for only one wavelengh, in other words for monochromatic waves alone.

Now,

$$z_0 \equiv \frac{k_\perp V_o}{\Omega}$$

and phase velocity, v_{ph}, is given by

$$v_{ph} = \frac{\omega}{k_\perp}$$

for $k_\parallel = 0$.

Therefore z_0 can be written as

$$z_0 \equiv \frac{\omega}{\Omega} \frac{V_o}{v_{ph}}$$

For $\omega/\Omega = (2n+1)/2$ instability occurs for

$$\frac{v_{ph}}{V_0} \simeq \frac{2n+1}{2} \left(\frac{1}{z_0}\right)_{crit.}$$

or

$$\frac{v_{ph}}{V_0} \simeq \frac{2n+1}{2} A\left(\frac{1}{k_\perp}\right)_{crit.} \qquad (\text{IV}.1)$$

where A is a constant and $(k_\perp)_{crit.}$ is the most unstable $k_\perp$.

It will be shown that $(z_0)_{crit.}$ depends on both ω_p and the parameters of the distribution function.

It can be seen from figure (IV. 1) that instability will occur at or near integral values of $n > 1$.

So provided that

$$V_0 < v_{ph} < V_2$$

the unstable bands would occur at values given by (IV. 1) and would have width for which the value of v_{ph}/V_0 does not exceed

$$\left(\frac{2n-\epsilon+1}{2}\right)\left(\frac{1}{z_0}\right)_{crit} \leqslant \frac{v_{ph}}{V_0} \leqslant \left(\frac{2n+\epsilon+1}{2}\right)\left(\frac{1}{z_0}\right)_{crit}$$

where ϵ is a small number, $0 \leqslant \epsilon < 1$, determining the unstable band width in z_0.

The next factor that instability depends upon is the relative velocity spread. To investigate this V_2/V_0 was kept constant.

It was found that as $(V_2-V_1)/V_0$ increases the onset of instability shifts to higher values of z_0. See figures (IV. 6) and (IV. 7). That means that as the velocity spread increases instability becomes possible for smaller wavelengths.

Increasing spread in the velocity means that the curve of $\int f dv_{\parallel}$ versus $v_{\perp}$ becomes flatter and that the number of particles with a given $v_{\parallel}$ cover a greater range of $v_{\perp}$ velocities.

It was further found that the critical plasma density increases, $(\Omega/\omega_p)^2$ decreases, for increasing values of $(V_2-V_1)/V_0$.

Part of the variation of $(\Omega/\omega_p)^2$ with $(V_2-V_1)/V_0$ is plotted in figure (IV. 8) for three different values of the ratio V_2/V_0 for the respective first critically stable band of each ratio.

In figure (IV. 4) there is a qualitative plot for two different values of V_2/V_0 showing the complete curve.

Considering the right hand side of the curves of figure (IV. 4) plotted accurately in figure (IV. 8) we can see that as $(V_2-V_1)/V_0$ increases $(\Omega/\omega_p)^2$ tends to zero, faster for smaller values of V_2/V_0, and the plasma is always stable for infinite plasma density.

Conversely, as $(V_2-V_1)/V_0$ decreases $(\Omega/\omega_p)^2$ tends to an upper limit and then as $V_1 \rightarrow V_2$, i.e. with still decreasing $(V_2-V_1)/V_0$, $(\Omega/\omega_p)^2$ starts deacreasing tending to zero.

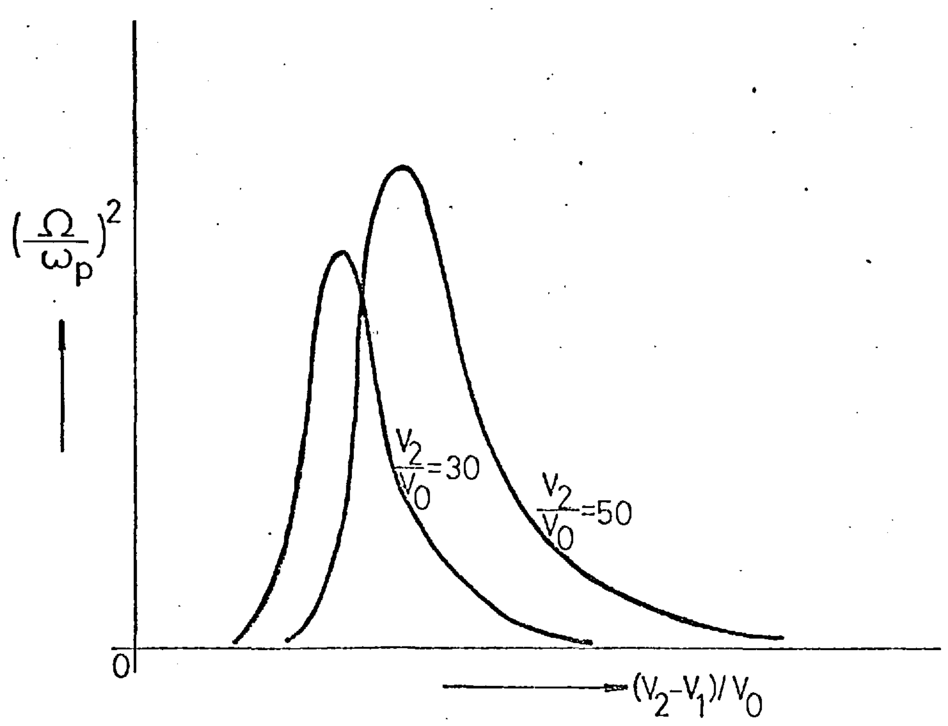

Figure (IV. 4)
Variation of $(\Omega/\omega_p)^2_{crit}$ with $(V_2-V_1)/V_0$

Further, the behaviour of z_0 and $w_{min.}$ was investigated at minimum critical plasma density with increasing velocity spread. It was found that $(w_{min})_{crit}$ increases to a maximum value and then falls again, its range however never exceeding $1.4 \leqslant (w_{min})_{crit} \leqslant 1.5$. Whereas $(z_0)_{crit}$ increases continuously with increasing $(V_2-V_1)/V_0$; see table (IV. 1).

The last point to look at was the behaviour of the function with increasing values of V_2/V_0 and the same velocity spread.

It was found that as V_2/V_0 increases the onset of instability shifts to lower values of z_0 and the band width decreases very markedly. See figures (IV. 9), (IV. 10) and (IV. 11). This is not a surprising result since it implies that instability would be possible for greater values of

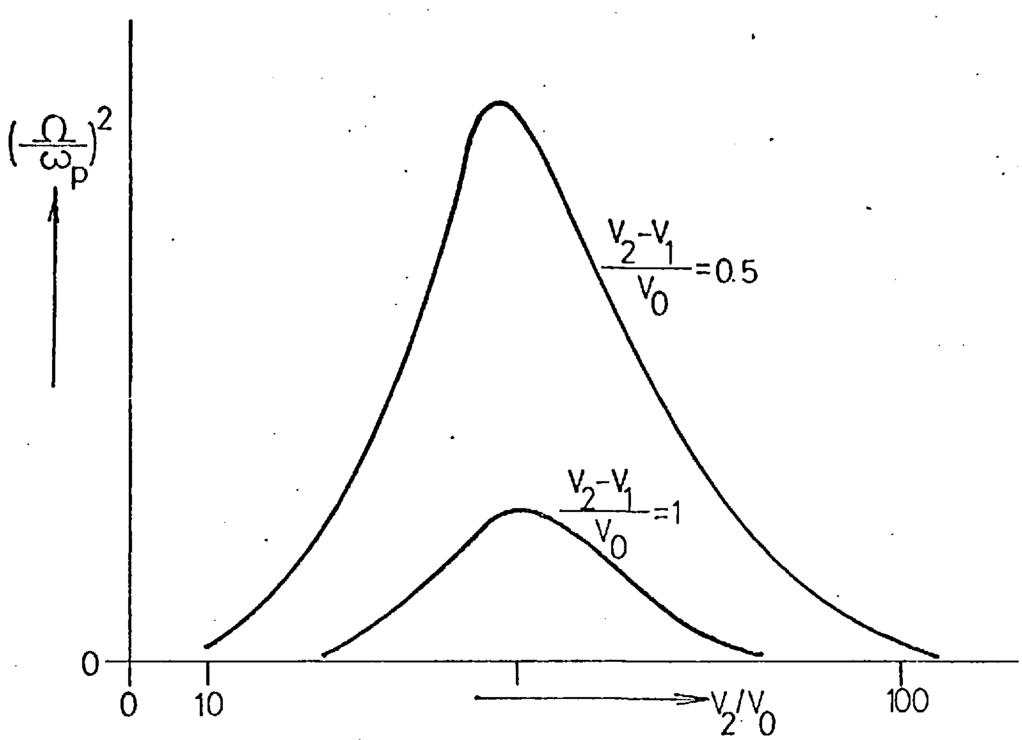

Figure (IV.5)
Variation of $(\Omega/\omega_p)^2$ with V_2/V_0

the phase velocity.

Looking at the critically stable bands it was found that with increasing V_2/V_0 the minimum critical plasma density decreases down to a minimum value, see figure (IV. 5) and then with still increasing V_2/V_0 the critical density increases thereby the plasma becoming stable.

Figure (IV. 12) is part of the left hand side of figure (IV. 4) plotted accurately.

The corresponding behaviour of $w_{min.}$ and z_0, at critical plasma density, with increasing V_2/V_0, is illustrated in figure (IV. 13). It can be seen that as V_2/V_0 increases $w_{min.}$ decreases down to a minimum value and then increases again whereas $(z_0)_{crit}$ decreases monotonically with increasing V_2/V_0. At approximately $(V_2/V_0)=100$, $(z_0)_{crit}$ has reached a value of approximately 0.2 which is the limit for critical stability. At $V_2/V_0 > 100$, $(V_2-V_1)/V_0=0.5$ only stable solutions are possible. See also the appendix.

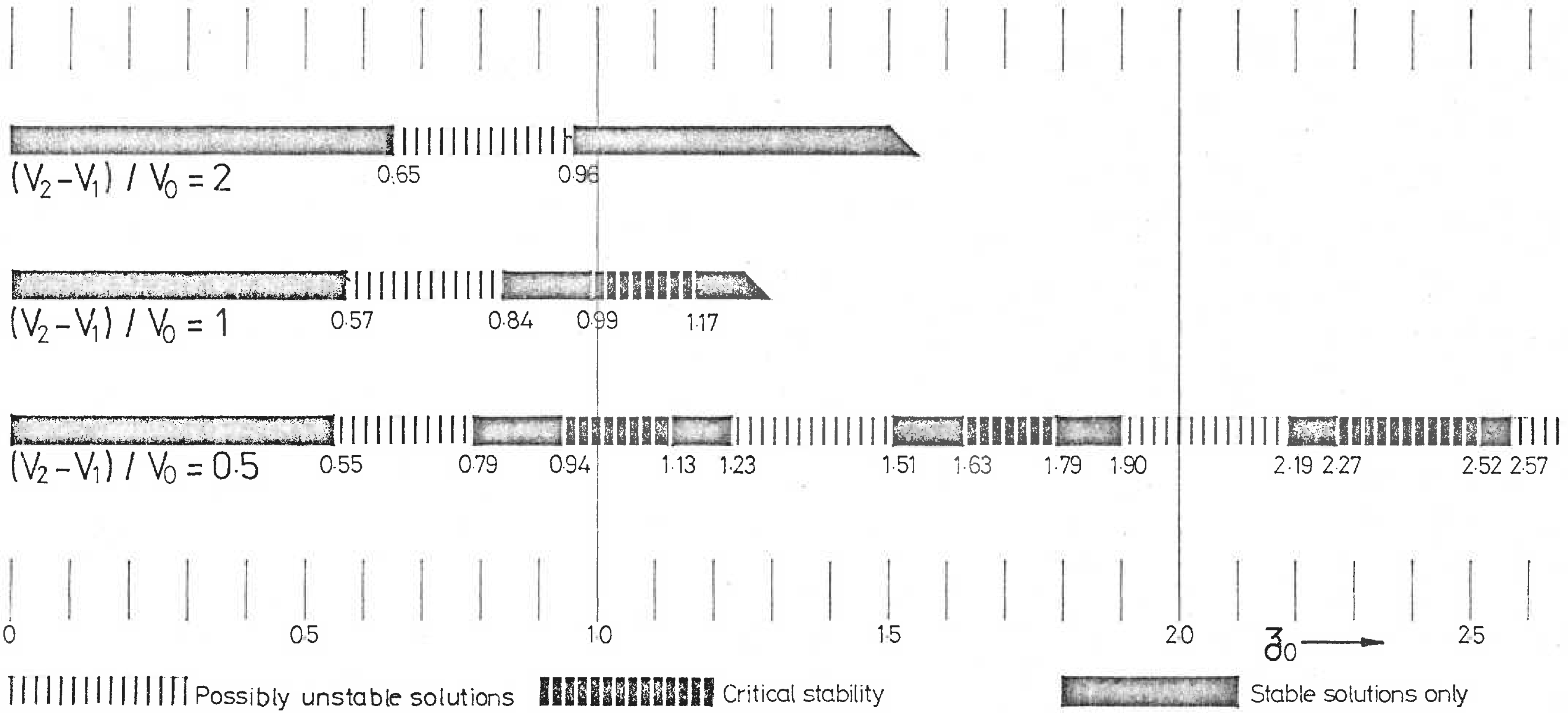

Figure (IV·6)

Band structure of unstable solutions of the dispersion relation for increasing $\mathfrak{z}_0$.
Distribution functions plotted have the same $V_2/V_0 = 5$ ratio but different thermal spread to pitch-angle ratios.

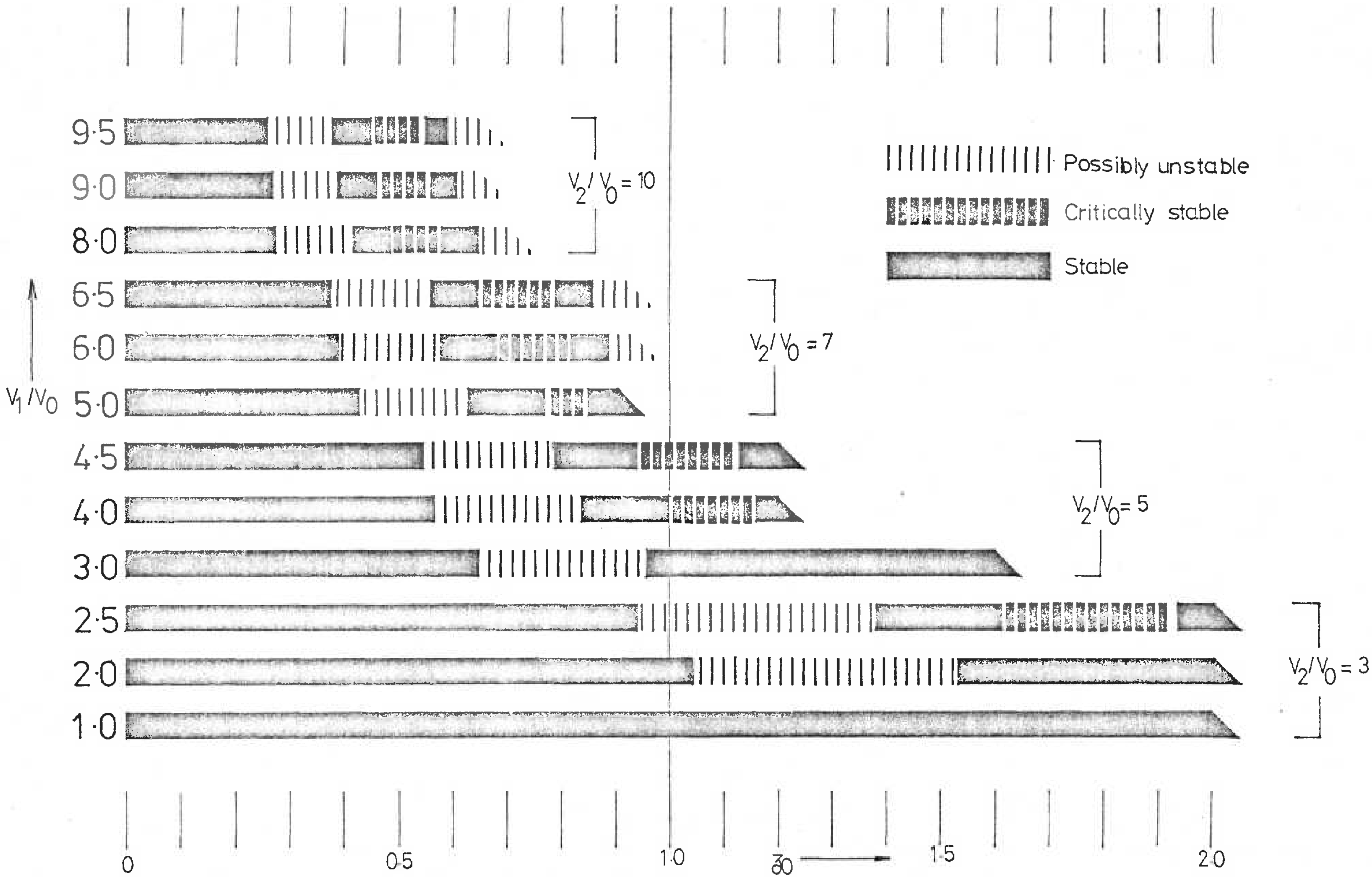

Figure (IV·7)
Band structure of the solutions of the dispersion relation for increasing z_0 and for various values of the distribution function

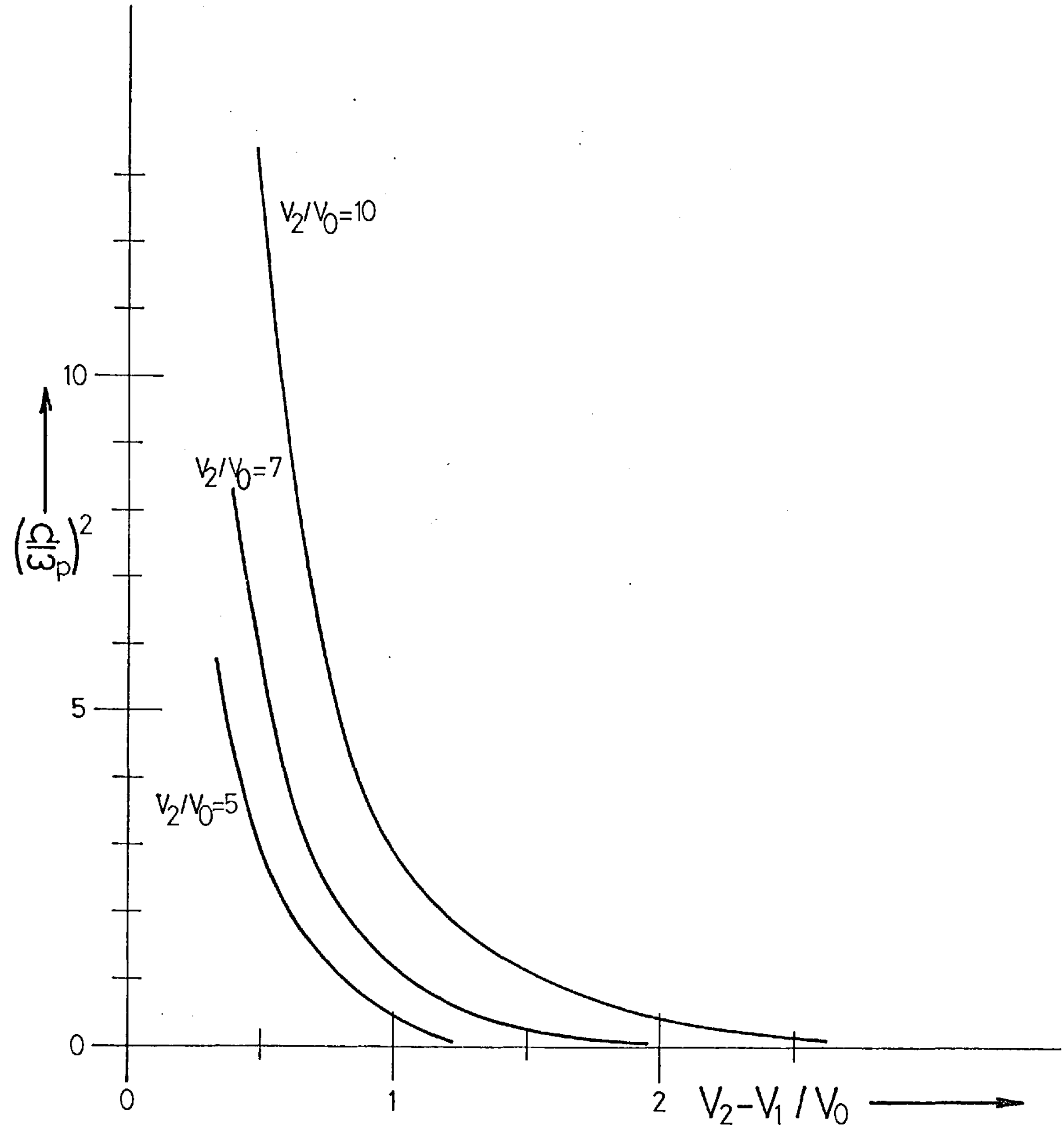

Figure (IV·8)
Variation of minimum $(\Omega/\omega_p)^2$ with V_2-V_1/V_0 for different values of V_2/V_0

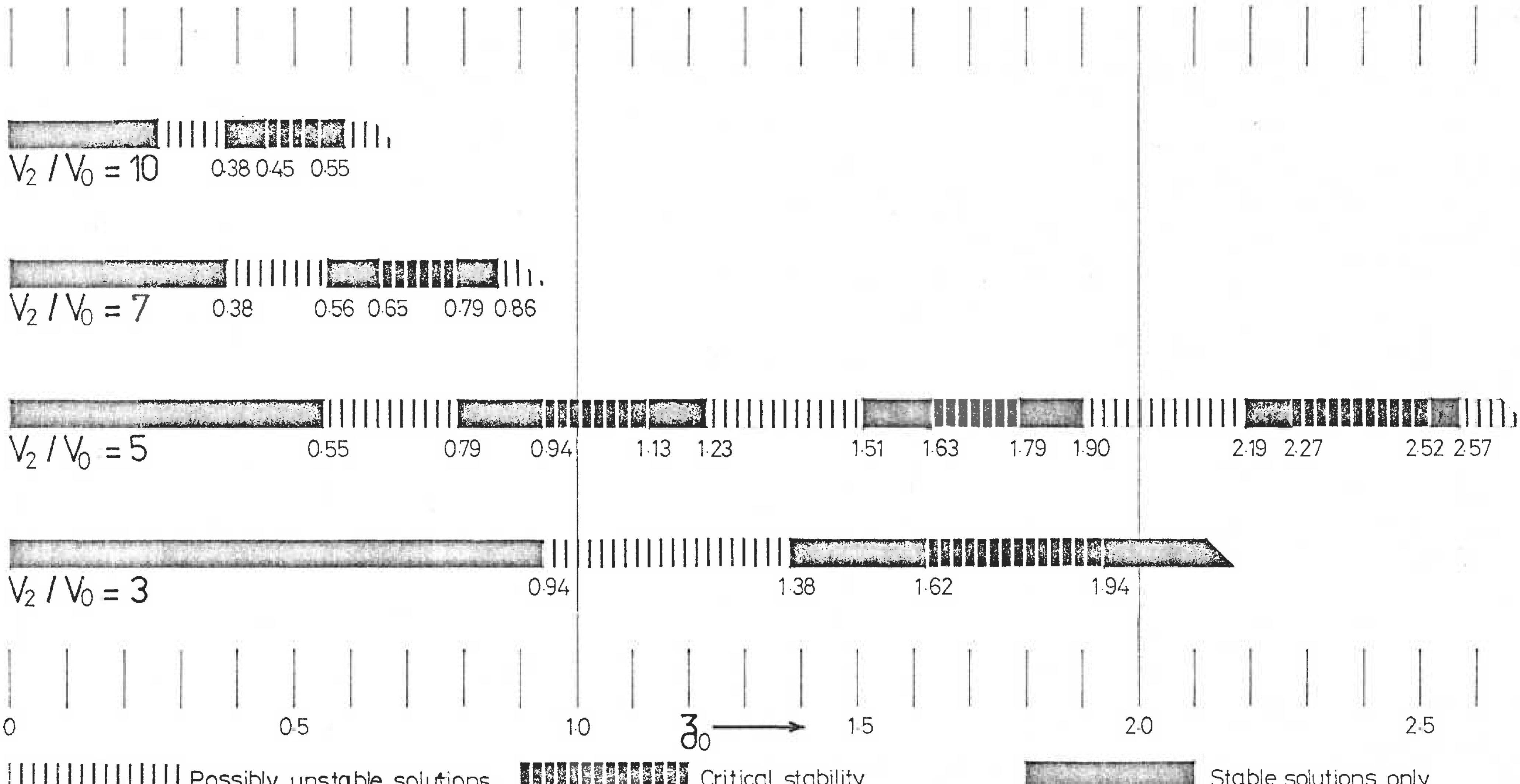

Figure (IV·9)

Band structure of unstable solutions of the dispersion relation for increasing ζ_0
Distribution functions plotted have the same thermal spread to pitch-angle ratio, $(V_2 - V_1)/V_0 = 0.5$ but different V_2/V_0 ratios

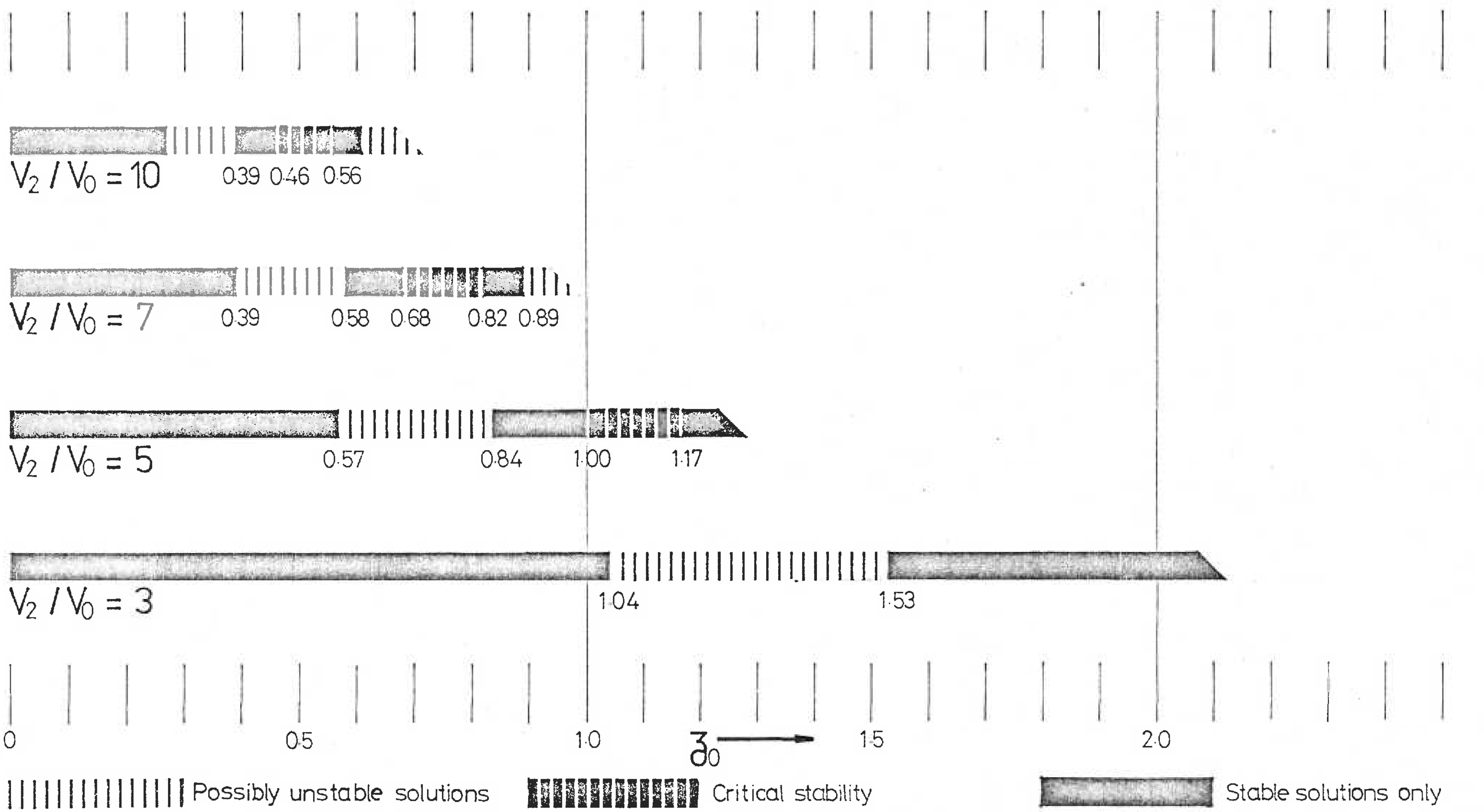

Figure (IV · 10)

Band structure of unstable solutions of the dispersion relation for increasing $ʒ_0$
Distribution functions plotted have the same thermal spread to pitch-angle ratio, $(V_2 - V_1)/V_0 = 1$, but different V_2/V_0 ratios

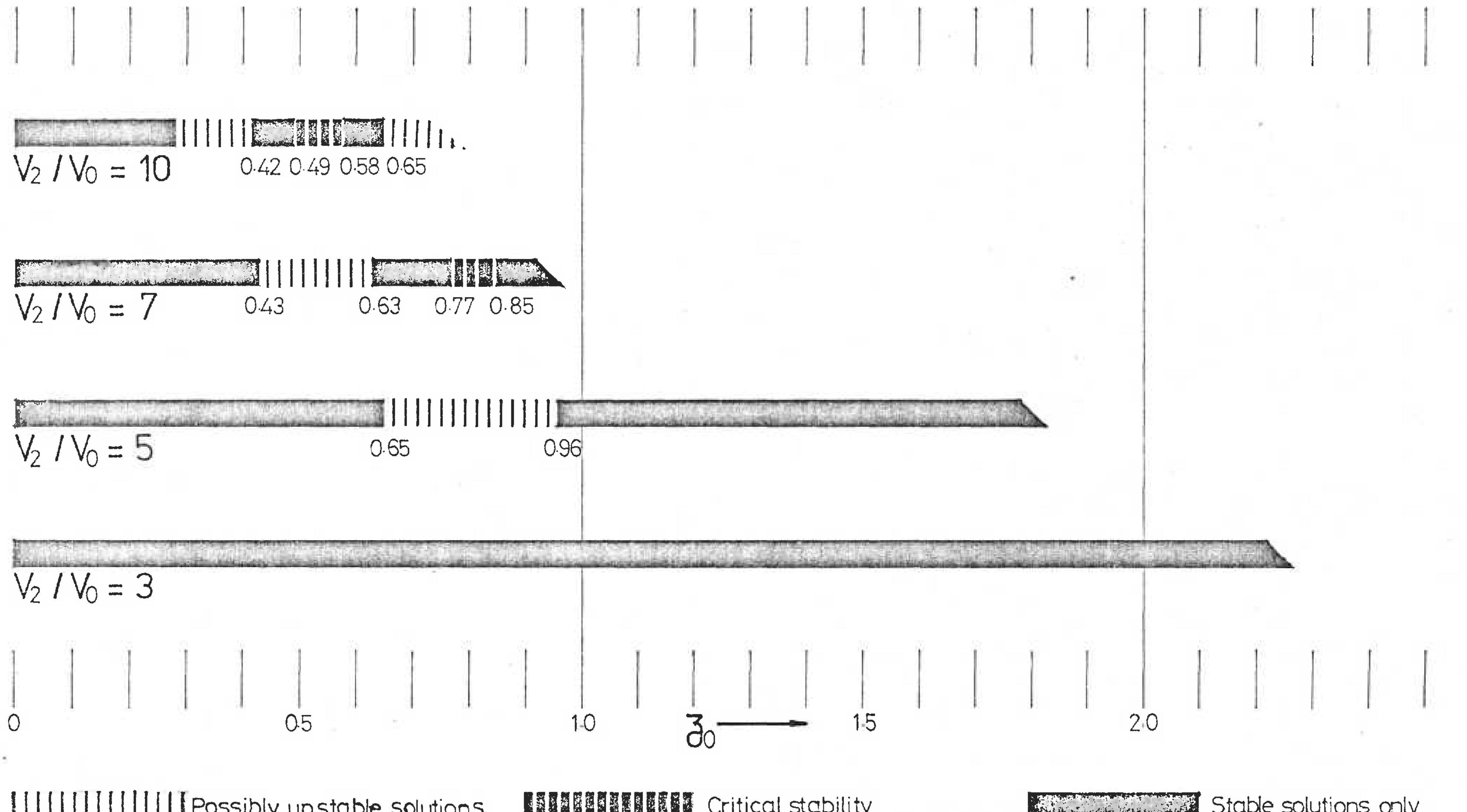

Figure (IV·11)

Band structure of unstable solutions of the dispersion relation for increasing ζ_0
Distribution functions plotted have the same thermal spread to pitch-angle ratio, $(V_2-V_1)/V_0 = 2$, but different V_2/V_0 ratios

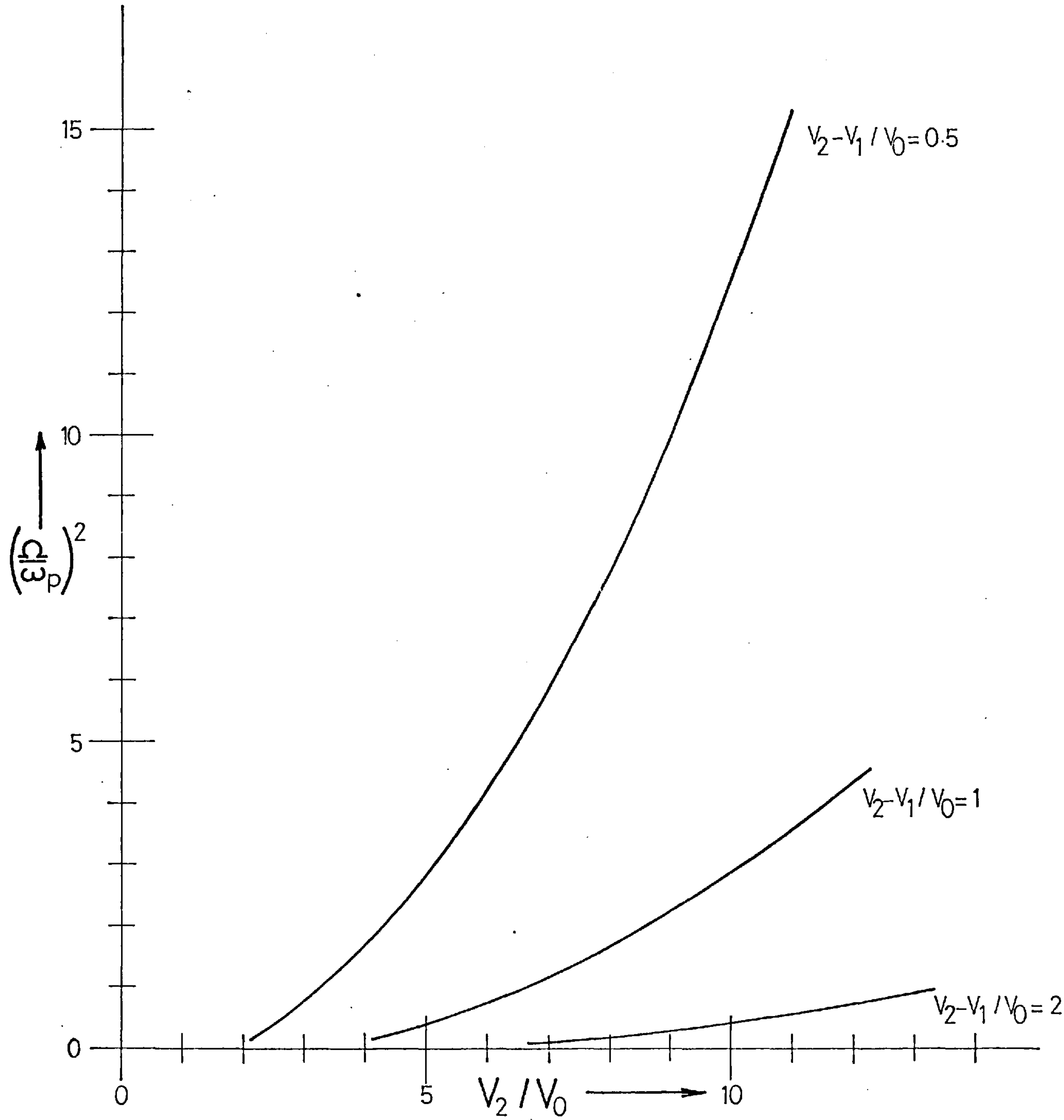

Figure (IV·12)

Variation of minimum $(\Omega / \omega_p)^2$ with V_2/V_0 for different values of $V_2 - V_1 / V_0$

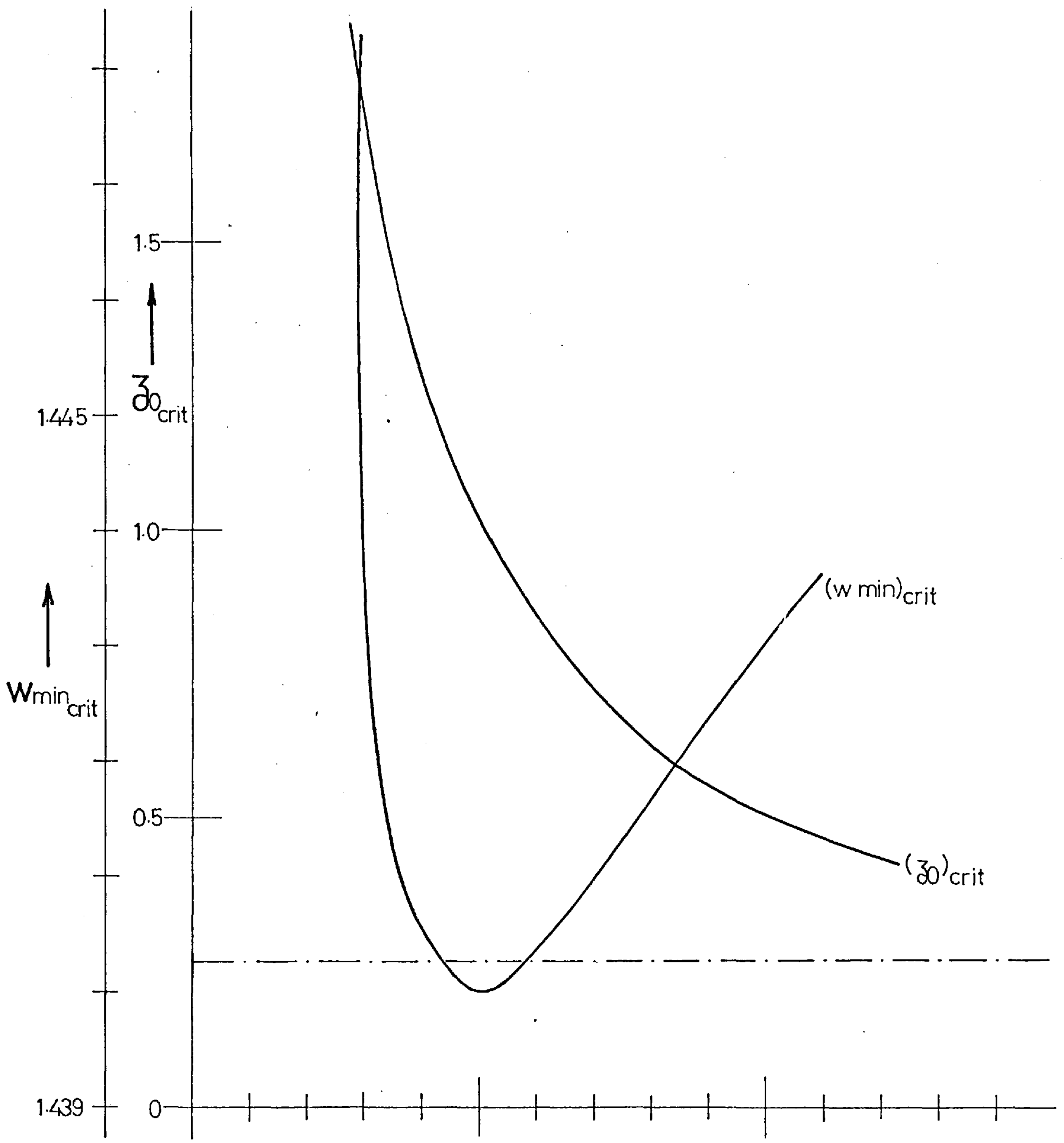

Figure (IV·13)
Variation of $(\mathfrak{z}_0)$crit and (w min)crit with V_2/V_0 for the same V_2-V_1/V_0 ratio

$\frac{(V_1)}{(V_0)}$	$\frac{(V_2)}{(V_0)}$	$\frac{(V_2-V_1)}{(V_0)}$	$(z_0)_{crit}$	$(w_{min})_{crit}$	$\frac{(\Omega)^2}{(\omega_p)^2_{min}}$
2.5	3	0.5	1.76	1.448	0.8
4.0	5	1.0	1.08	1.442	0.4
4.5	5	0.5	1.02	1.440	2.8
5.0	7	2.0	0.81	1.441	0.1
6.0	7	1.0	0.75	1.443	1.1
6.5	7	0.5	0.72	1.441	5.8
8.0	10	2.0	0.54	1.440	0.4
9.0	10	1.0	0.51	1.439	2.8
9.5	10	0.5	0.50	1.443	12.4

Table (IV. 1)

Some typical values obtained for the variation of the minimum value of the critical plasma density and the corresponding values of z_0 and w_{min} at which it occurs with various parameters of the distribution function. All values shown are for the first critically stable band of each value of the velocity distribution function.

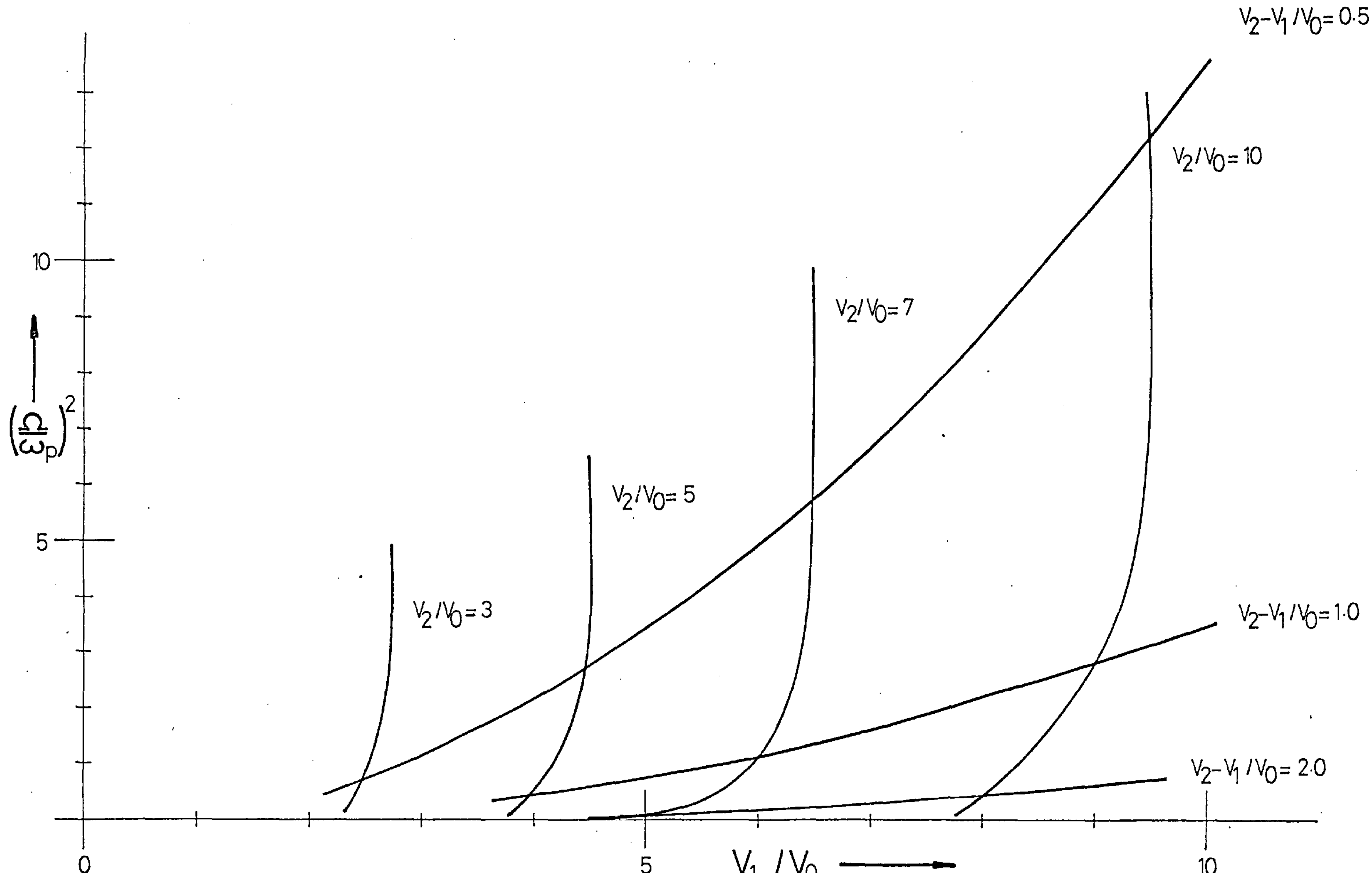

Figure (IV·14)

Variation of minimum critical $(\Omega/\omega_p)^2$ with V_1/V_0 for given V_2/V_0 or $V_2 - V_1/V_0$

The minimum value of $(\Omega/\omega_p)^2$ is given by the points of intersection of the V_2/V_0 with the $V_2 - V_1/V_0$ curves

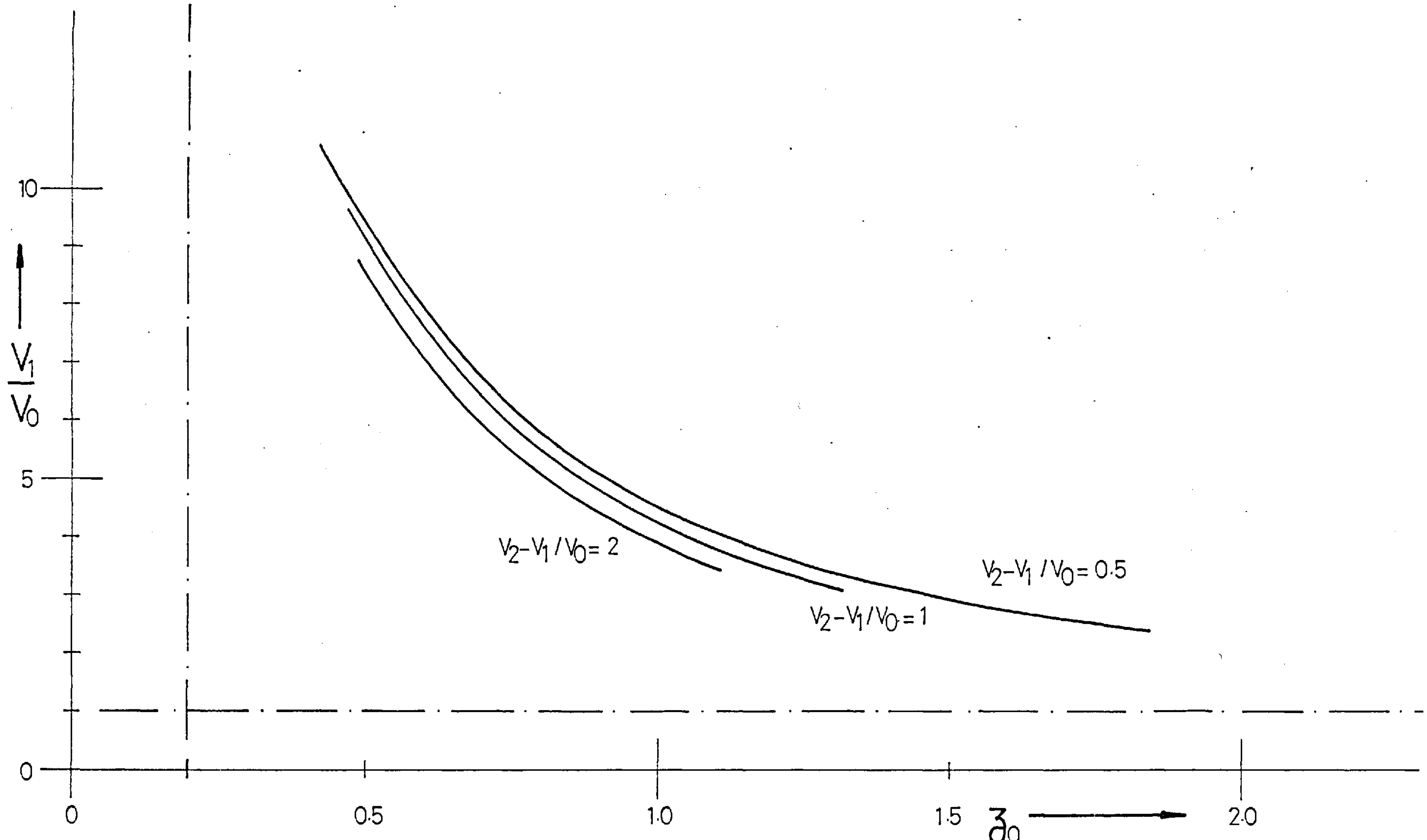

Figure (IV · 15)
Variation of V_1/V_0 with $\mathfrak{z}_0$ at minimum critical plasma density

(V). SUMMARY OF RESULTS

(a). CONDITIONS FOR CRITICAL STABILITY.

It is useful at this point to summarize the general conditions that have to be fulfilled to obtain unstable mode solutions. How the parameters of the distribution function affect instability will be discussed in the next subsection.

For any parameters of the hollow distribution function critical stability is only possible for a given frequency spectrum and a given wavelength range.

Unstable solutions are bound by maximum and minimum values of the wavelength which depend very strongly on the relative perpendicular velocity spread and the maximum perpendicular velocity to pitch-angle ratio of the velocity distribution function.

The frequency spectrum of these unstable modes is remarkably constant always lying within $1.4 \leqslant \omega/\Omega \leqslant 1.5$. Further, for a given wavelength and distribution function unstable modes are also bound by a minimum value of the plasma frequency. In general the following relationship holds. As the wavelength decreases the minimum value of the plasma frequency increases, so that, for sufficiently short wavelength $\omega_p \to \infty$ and the plasma is always stable.

The word sufficiently is used since the value of the minimum wavelength is a function of the parameters of the velocity distribution function.

Conversely, as the wavelength tends to infinity no instability is possible whatever the parameters of the distribution function or for any plasma frequency.

(b). DEPENDENCE OF THE VALUES OF ω_p, z_0, $w_{min.}$ AT CRITICAL PLASMA DENSITY ON THE PARAMETERS OF THE DISTRIBUTION FUNCTION.

It was found that as $(V_2-V_1)/V_0$ increases the onset of instability moves to shorter wavelengths whereas V_2/V_0 increases instability becomes possible for longer wavelengths.

Now, with reference to figure (IV. 4) it can be seen that the critical plasma density becomes infinite as $V_1 \rightarrow V_2$ and as $V_1 \rightarrow V_0$. So instability is possible only if

$$V_0 < V_1 < V_2$$

The value of the critical plasma density, however, decreases monotonically with increasing V_2/V_0.

Considering now the behaviour of critical ω_p with the ratio V_2/V_0 we can see from figure (IV. 5) that instability is possible within a given range of V_2/V_0 only and that this range depends on the relative velocity spread. The larger the spread the smaller the range of V_2/V_0 for which instability is possible and the larger the value of the minimum critical plasma density.

Furthermore it was found that as V_2/V_0 tends to its maximum value the band width in $k_\perp$ decreases and critical stability is possible only for a single wavelength.

For a given velocity spread instability is bound by a lower limit in V_2/V_0,

$$1 < V_2/V_1 < V_2/V_0$$

but provided the above inequality is satisfied instability seems to be possible for arbitrary large values of V_2/V_0.

We can now state the general condition that the distribution function must satisfy for critical stability.

Plasma is always stable as $V_1 \to V_2$ or $V_1 \to V_0$. If however inequalities (V .1) are always satisfied simultaneously the plasma is unstable.

$$V_0 < V_1 < V_2$$
$$1 < \frac{V_2}{V_1} < \frac{V_2}{V_0} \qquad \text{(V. 1)}$$

At this point it is perhaps informative to look at the variation of $(\Omega/\omega_p)^2$ with V_1/V_0.

Referring to figure (IV. 14) which is part of the total curves of figures (IV. 4) and (IV. 5) we can see that the critical plsma density decreases with increasing V_2/V_0 and decreasing $(V_2-V_1)/V_0$ down to a minimum and then starts increasing again.

From figure (IV. 14) we can see that when the curves of constant $(V_2-V_1)/V_0$ and V_2/V_0 are drawn, their intersections give the value of the critical plasma density for that distribution function and that as $V_1/V_0 \to 1$ the curves can only intersect at zero $(\Omega/\omega_p)^2$ or in other words the plasma is stable.

If we compare the last point mentioned above with figure (IV. 15) that illustrates the variation of V_1/V_0 with $(z_0)_{crit}$ it will be seen that as V_1/V_0 approaches asymptotically to 1, $(k_\perp)_{crit}$ approaches infinity and consequently the plasma is stable.

Conversely as V_1/V_0 approaches infinity $(z_0)_{crit}$ approaches the value of approximately 0.2 below which only stable mode solutions are possible. Actually this is the absolute minimum value for which instability is at all possible. Below this value the coefficients of the Bessel functions, I_1 and I_2, have always the same sign and thereby only stable Bernstein modes are obtained.

In general, however, with increasing V_1/V_0 ratio, the onset of instability moves to longer wavelengths.

The variation of $(w_{min})_{crit}$ and $(z_0)_{crit}$ with increasing V_1/V_0 are illustrated in figure (V. 1) and figure (IV. 15) respectively. It can be seen that as V_1/V_0 increases $(w_{min})_{crit}$

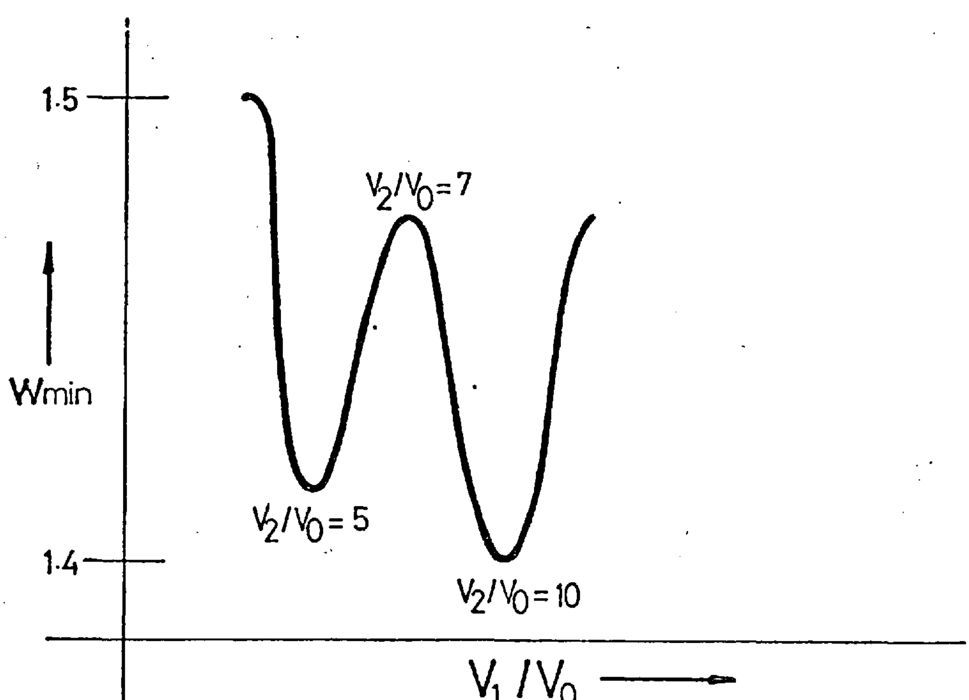

Figure (V. 1)
Diagram illustrating the variation of V_1/V_0 with w_{min}.
Each peak gives w_{min} at minimum critical density for a particular value of V_2/V_0

oscillates with frequency given by the ratio of the successive values of V_2/V_0 , see also figure (IV. 13) and amplitude, varying between $1.4 \leqslant w_{min} \leqslant 1.5$, determined by the relative velocity spread.

A discussion of the results and the way they are related to observations will now follow.

(VI) DISCUSSION ON THE RESULTS AND SOME RELATED OBSERVATIONS

The emissions at $\omega=(n+\frac{1}{2})\Omega$ were first observed by Alouette II, H. Oya (1971) and then by OGO 5, F. L. Scarf and R. W. Fredricks (1971).

In the Alouette II ionospheric experiments the sounder antenna emits a pulse which can stimulate wave emissions one type of which is the $(3/2)\Omega$-wave. These modes disappear (2 - 20)msec. after the sounder pulse.

Where the above unstable modes are locally stimulated, OGO 5 detected similar waves occuring "naturally", i.e. due to magnetospheric processes, at $L\simeq(4 - 10)$ and MLAT $\leqslant 10^{\circ}$. It is perhaps of some interest to note that $L\simeq 10$ is one of the possible points where the triggering mechanism of a magnetic substorm is believed to start and $L\simeq 4$ is the inner limit to which the influence of minor magnetic disturbances, due to fluctuations occuring at large L, is felt.

The $(3/2)\Omega$-emissions observed by OGO 5, appear to be correlated with magnetic substorms and simultaneous but distant precipitation events on nearly the same L-shells. In contrast to the Alouette events, these waves persist for minutes or hours.

It is conceivable that both the Alouette and OGO 5 observations arise due to equivalent plasma conditions.

If the trigger-pulse produces turbulence in the plasma leading to an anisotropic velocity distrbution of the particles, unstable modes can result. Similarly, it is possible that magnetospheric processes, occuring at the night-side auroral zones of the earth during magnetic substorms, can produce a similar type of anisotropic velocity distribution of the electrons and subsequent instability.

Experimental evidence suggests that these emissions are the result of non-linear processes in the plasma since, for instance, the transmitter has no frequency component in its spectrum which is selectively favourable at the $(3/2)\Omega$ frequencies (Oya, 1971).

On using the scalar dispersion relation one can allow for the non-linearity of the process by taking a distorted velocity distribution function for the electron velocities.

It was found by direct observation (Scarf & Fredricks, 1971), and by numerical calculations based on observations (Oya, 1971) that a velocity anisotropy in the distribution of the electrons preceeds the emission of the $(3/2)\Omega$-waves. Some details of the OGO 5 observations relating to this point were discussed briefly in chapter (II.a). For the locally stimulated emissions Oya found by a numerical calculation based on his observations of the Alouette II ionograms that electrons are accelerated in a direction perpendicular to $\underline{B}_o$, whereas they are decelerated in a direction parallel to $\underline{B}_o$ and that the plasma energy is increased by approximately 2 to 86 times the unperturbed energy, depending on the value of ω/Ω and that consequently there exists an anisotropy between the perpendicular and parallel electron energy.

These observations seem to be in agreement with the results obtained from this theoretical analysis, namely that instability is initiated and maintained as a result of an anisotropic velocity distribution function and that as the distribution function tends toward isotropy or becomes non-hollow, see chapter V, at the limiting cases of $V_I \to V_0$ or $V_I \to V_2$, instability is not possible.

It was also shown in chapters IV and V that this instability depends very critically on $\omega_p, k_\perp$ and the value of f_0.

It was reported both by Scarf & Fredricks and Oya that strong emissions with frequency ratio, ω/Ω, between $1.3 \leqslant \omega/\Omega \leqslant 1.9$ exist only when $2.2 \leqslant \omega_p/\Omega \leqslant 3.6$ and that these waves could not be identified at all when $\omega_p/\Omega < 1.8$. This observation seems to be in agreement with results of this work where it was found that instability is bound by a minimum value of the plasma frequency. Referring to figures (IV. 1), (IV. 4) and table (IV. 1) we can see that this minimum value would depend on the parameters of the distribution function.

Oya also reported that he could not detect any $(3/2)\Omega$ waves when $\omega_p/\Omega > 6.8$ but he remarks that this upper limit may be due to insufficient frequency resolution of the instrument.

Further observations by Nelms and Lockwood (1966), Scarf and Fredricks and Oya, confirm by observation the following points.

(1). That the $(2n+1)\Omega/2$ -waves have groups of frequency ranges clearly separated from eachother.

(2). That these waves have enhanced amplitudes near $\omega=1.5\Omega$ and that this value depends on the local plasma parameter (ω_p/Ω), c.f. figure (IV.1).

(3). The frequency spectrum, which is fairly broad and the time duration of these emissions are strongly dependent on ω_p/Ω and moreover the time duration depends also on the ratio ω/Ω, being 3-5 times larger in the frequency range $1.5 \leqslant w \leqslant 1.63$ than in the other portion of the observed frequency range. Compare this with figure (IV.3).

(4). The time duration and intensity of the emissions falls with increasing value of n, n referring to the formula $(2n+1)\Omega/2$.

(5). There are two weaker emissions (not observed at the same time, Oya 1971), one on the high frequency side and the other on the low frequency side of the main branch. I am not quite sure if this observation correlates with the "bands" in k, compare figures (IV.1) and (IV.2), discussed in chapter IV, but it seems a possible hypothesis.

(VII). CONCLUSIONS

From the examination of this theoretical work and other experimental data, we can see that:

(1). Electrostatic emissions with frequency $\omega \simeq (2n+1)\Omega/2$ exist as a result of non-linear effects, operative in the magnetospheric plasma, which produce unstable anisotropic velocity distributions in the particle populations;

(2). These emissions are separated from eachother by definite gaps both in their frequency and their wavelength;

(3). The unstable modes are bounded both in frequency and wavelength;

(4). Critical stability depends very strongly on $\omega_p, k_\perp$ and the parameters of the distribution function and unstable mode solutions cannot exist outside given limiting values of the above variables;

(5). The problem of non-linearity which leads to anisotropic distributions and the subsequent interactions of these waves to produce isotropy and precipitation has not so far been solved.

Previous theories to the present one which attempted an explanation tackled the problem either as a linear one with δ-function distributions, Fredricks (1971), or as a quasi-linear 3-wave interaction based on the weak plasma-turbulance treatment of Kadomtzev, Oya (1971). It would perhaps prove to be a rather interesting , even if somewhat messy theoretical problem,to attempt a complete non-linear treatment starting by general wave-equations and to treat the problem as a stochastic process.

APPENDIX 1.

Case of $k_\perp \to 0$

We shall investigate what happens to the scalar dispersion relation as the argument of the Bessel functions, z_0 tends to zero.

For finite $v_\perp$ and $\Omega \neq 0$ when $z_0 \to 0$ that means that $k_\perp$ tends to zero.

Throughout this section the following definitions will hold.

$$z \equiv \frac{k_\perp v_\perp}{\Omega}$$

$$z_0 \equiv \frac{k_\perp V_0}{\Omega} \qquad (1)$$

$$\frac{V_2 - V_1}{V_0} \equiv x_0$$

$$\frac{V_2}{V_1} \equiv y_0 .$$

$$(y_0 - x_0) \equiv r_0$$

The series representation of the Bessel function of the first kind, $J_n(z)$, is,

$$J_n(z) = \sum_{r=0}^{\infty} \frac{(-1)^r (\frac{1}{2} z)^{n+2r}}{\Gamma(\nu+r+1) r!} \qquad (2)$$

where $\Gamma(\nu) = (\nu - 1)!$

The function I_n defined in (III.5) by using the equation (II.8) can be written as:

$$I_n = nZ + \frac{1}{2}(Y1+Y2) \qquad (3)$$

and where

$$Z = n\left[z_0(y_0^2-1)^{1/2} - z_0(r_0^2-1)^{1/2}\right]J_n^2(z_0)$$

$$Y1 = \frac{1}{2}\int_{z_0 r_0}^{z_0 y_0}\left(J_{n-1}^2(z) - J_{n+1}^2(z)\right)\left(z_0^2y_0^2 - z^2\right)^{1/2} z\,dz \qquad (3a)$$

$$Y2 = \frac{1}{2}\int_{z_0}^{z_0 r_0}\left(J_{n-1}^2(z) - J_{n+1}^2(z)\right)\left[\left(z_0^2y_0^2 - z^2\right)^{1/2} - \left(z_0^2r_0^2 - z^2\right)^{1/2}\right] z\,dz$$

We shall compare the coefficients I_1 and I_2 using the above relation to see whether instability is possible.

Using equation (2) and ignoring terms in z of power greater than 4 we have

$$J_0(z) = 1 - \left(\frac{z}{2}\right)^2 + \left(\frac{z/2}{4}\right)^4$$

$$J_1(z) = \left(\frac{z}{2}\right) - \left(\frac{z/2}{2}\right)^3$$

$$J_2(z) = \left(\frac{z}{2}\right)^2 - \left(\frac{z/2}{6}\right)^4 \qquad (4)$$

and

$$J_0^2(z) = 1 - \frac{z^2}{2} + \frac{6z^4}{64}$$

$$J_1^2(z) = \frac{z^2}{4} - \frac{z^4}{16}$$

$$J_2^2(z) = \frac{z^4}{64}$$

Now for $n=0$, $Z=Y1=Y2=0$, see equation (II.8) and need not concern us. We then choose in the first instance a particular distribution function with $y_0=5$ and $r_0=4.5$ and obtain;

For n=1.

$$Z = z_0\left[(y_0^2-1)^{1/2} - (r_0^2-1)^{1/2}\right]\left(\frac{z_0^2}{4} - \frac{z_0^4}{16}\right)$$

$$(y_0^2-1)^{1/2} = 4.89$$

$$(r_0^2-1)^{1/2} = 4.46$$

$$\therefore\ Z = 0.43 z_0\left(\frac{z_0^2}{4} - \frac{z_0^4}{16}\right)$$

$$Z = \frac{0.43}{4} z_0^3\left(1 - \left(\frac{z_0}{2}\right)^2\right) \qquad (a)$$

$$Y1 = \frac{1}{2}\int_{z_0 r_0}^{z_0 y_0}\left(1 - \frac{z^2}{2} - \frac{6z^4}{64} - \frac{z^4}{64}\right)(z_0^2 y_0^2 - z^2)^{1/2} z\,dz$$

$$= \frac{1}{2}\int_{z_0 r_0}^{y_0 z_0}\left(z - \frac{z^3}{2} + \frac{5}{64}z_0^5\right)(y_0^2 z_0^2 - z_0^2)^{1/2}\,dz$$

In general the following relationships hold:

$$\left.\begin{aligned}
\int_{\epsilon}^{\alpha} x(\alpha^2-x^2)^{1/2}dx &= \frac{1}{3}(\alpha^2-\epsilon^2)^{3/2}\\
\int_{\epsilon}^{\alpha} x^3(\alpha^2-x^2)^{1/2}dx &= -\frac{1}{5}\alpha^5\frac{(\alpha^2-\epsilon^2)^{1/2}}{\alpha}\left[\left(\frac{\epsilon}{\alpha}\right)^4 - \frac{1}{3}\left(\frac{\epsilon}{\alpha}\right)^2 - \frac{2}{3}\right]\\
\int_{\epsilon}^{\alpha} x^5(\alpha^2-x^2)^{1/2}dx &= -\frac{1}{7}\alpha^7\frac{(\alpha^2-\epsilon)^{1/2}}{\alpha}\left[\left(\frac{\epsilon}{\alpha}\right)^6 - \frac{1}{5}\left(\frac{\epsilon}{\alpha}\right)^4 - \frac{4}{15}\left(\frac{\epsilon}{\alpha}\right)^2 - \frac{8}{15}\right]
\end{aligned}\right\}(5)$$

Therefore Y1 becomes:

$$Y1 = \frac{1}{2}\left\{\int_{z_0r_0}^{z_0y_0} z\left(z_0^2y_0^2 - z^2\right)^{1/2} dz - \frac{1}{2}\int_{z_0r_0}^{z_0y_0} z^3\left(z_0^2y_0^2 - z^2\right)^{1/2} dz + \frac{5}{64}\int_{z_0r_0}^{z_0y_0} z^5\left(z_0^2y_0^2 - z^2\right)^{1/2} dz\right.$$

$$= \frac{1}{2}\left\{\frac{1}{3}z_0^3\left(y_0^2 - r_0^2\right)^{3/2} + \frac{1}{10}y_0^4z_0^5\left(y_0^2 - r_0^2\right)^{1/2}\left[\left(\frac{r_0}{y_0}\right)^4 - \frac{1}{3}\left(\frac{r_0}{y_0}\right)^2 - \frac{2}{3}\right] -\right.$$

$$\left.\frac{5}{448}y_0^6z_0^7\left(y_0^2 - r_0^2\right)^{1/2}\left[\left(\frac{r_0}{y_0}\right)^6 - \frac{1}{5}\left(\frac{r_0}{y_0}\right)^4 - \frac{4}{15}\left(\frac{r_0}{y_0}\right)^2 - \frac{8}{15}\right]\right\}$$

For $$\left(y_0^2 - r_0^2\right)^{1/2} = 0.69$$

and $$\frac{r_0}{y_0} = 0.9$$

$$Y1 = \frac{1}{6}(0.69)^3z_0^3 + \frac{1}{20}y_0^4z_0^5(0.69)\left[(0.9)^4 - \frac{1}{3}(0.9)^2 - \frac{2}{3}\right] -$$

$$\frac{5}{2\times 448}y_0^6z_0^7(0.69)\left[(0.9)^6 - \frac{1}{5}(0.9)^4 - \frac{4}{15}(0.9)^2 - \frac{8}{15}\right]$$

$$\frac{Y1}{2} = 0.547z_0^3 - 0.009y_0^4z_0^5 + 0.0004y_0^6z_0^7$$

$$\frac{Y1}{2} = 0.547z_0^3 - 5.62z_0^5 + 6.27z_0^7 \qquad (b)$$

To find Y2.

$$Y2 = \frac{1}{2}\int_{z_0}^{z_0r_0}\left(J_{n-1}^2(z) - J_{n+1}^2(z)\right)\left[\left(z_0^2y_0^2 - z^2\right)^{1/2} - \left(z_0^2r_0^2 - z^2\right)^{1/2}\right]z\,dz$$

$$= \frac{1}{2}\int_{z_0}^{z_0r_0}\left(1 - \frac{1}{2}z_0^2 + \frac{6}{64}z_0^4 - \frac{1}{64}z_0^4\right)\left[\left(z_0^2y_0^2 - z^2\right)^{1/2} - \left(z_0^2r_0^2 - z^2\right)^{1/2}\right]z\,dz$$

$$= \frac{1}{2}\int_{z_0}^{z_0r_0} z\left[\left(z_0^2y_0^2 - z^2\right)^{1/2} - \left(z_0^2r_0^2 - z^2\right)^{1/2}\right]dz -$$

$$\frac{1}{4}\int_{z_0}^{z_0r_0} z^3\left[\left(z_0^2y_0^2 - z^2\right)^{1/2} - \left(z_0^2r_0^2 - z^2\right)^{1/2}\right]dz +$$

$$\frac{5}{128}\int_{z_0}^{z_0 r_0} z^5\left[\left(z_0^2y_0^2-z^2\right)^{3/2}-\left(z_0^2r_0^2-z^2\right)^{1/2}\right]dz$$

Evaluating the integrals we obtain

$$Y2 = \frac{1}{2}\left[-\frac{1}{3}\left(y_0^2-r_0^2\right)^{3/2}z_0^3+\frac{1}{3}\left(y_0^2-1\right)^{1/2}z-\frac{1}{3}\left(r_0^2-1\right)^{3/2}z_0^3-\right.$$

$$\frac{1}{20}\left[z_0^5y_0^4\left(y_0^2-r_0^2\right)^{1/2}\left[\left(\frac{r_0}{y_0}\right)^4-\frac{1}{3}\left(\frac{r_0}{y_0}\right)^2-\frac{2}{3}\right]-z_0^5y_0^4\left(y_0^2-1\right)^{1/2}\left[\left(\frac{1}{y_0}\right)^4-\right.\right.$$

$$\left.\left.\frac{1}{3}\left(\frac{1}{y_0}\right)^2-\frac{2}{3}\right]+z_0^5r_0^4\left(r_0^2-1\right)^{1/2}\left[r_0^4-\frac{1}{3}r_0^2-\frac{2}{3}\right]\right]+$$

$$\frac{5}{128\times7}\left[z_0^7y_0^6\left(y_0^2-r_0^2\right)^{1/2}\left[\left(\frac{r_0}{y_0}\right)^6-\frac{1}{5}\left(\frac{r_0}{y_0}\right)^4-\frac{4}{15}\left(\frac{r_0}{y_0}\right)^2-\frac{8}{15}\right]-\right.$$

$$z_0^7y_0^6\left(y_0^2-1\right)^{1/2}\left[\left(\frac{1}{y_0}\right)^6-\frac{1}{5}\left(\frac{1}{y_0}\right)^4-\frac{4}{15}\left(\frac{1}{y_0}\right)^2-\frac{8}{15}\right]+$$

$$\left.z_0^7r_0^6\left(r_0^2-1\right)^{1/2}\left[\left(\frac{1}{r_0}\right)^6-\frac{1}{5}\left(\frac{1}{r_0}\right)^4-\frac{4}{15}\left(\frac{1}{r_0}\right)^2-\frac{8}{15}\right]\right]$$

We can see that Y1 cancels out the first terms in lines 1, 2 and 4. On rewriting therefore we obtain;

$$Y1+Y2 = \frac{1}{6}z_0^3\left[\left(y_0^2-1\right)^{3/2}-\left(r_0^2-1\right)^{3/2}\right]+\frac{1}{20}\left[z_0^5y_0^4\left(y_0^2-1\right)^{1/2}\right.$$

$$\left.\left[\left(\frac{1}{y_0}\right)^4-\frac{1}{3}\left(\frac{1}{y_0}\right)^2-\frac{2}{3}\right]-z_0^5r_0^4\left(r_0^2-1\right)^{1/2}\left[r_0^4-\frac{1}{3}r_0^2-\frac{2}{3}\right]\right]-$$

$$\frac{5}{128\times7}\left[z_0^7y_0^6\left(y_0^2-1\right)^{1/2}\left[\left(\frac{1}{y_0}\right)^6-\frac{1}{5}\left(\frac{1}{y_0}\right)^4-\frac{4}{15}\left(\frac{1}{y_0}\right)^2-\frac{8}{15}\right]-\right.$$

$$\left.z_0^7r_0^6\left(r_0^2-1\right)^{1/2}\left[\left(\frac{1}{r_0}\right)^6-\frac{1}{5}\left(\frac{1}{r_0}\right)^4-\frac{4}{15}\left(\frac{1}{r_0}\right)^2-\frac{8}{15}\right]\right]$$

Evaluating Y1+Y2 for the particular distribution function we obtain,

$$Y1+Y2 = \frac{1}{6}\left[(4.89z_0)^3-(4.46z_0)^3\right]+\frac{1}{20}\left[(5z_0)^4(4.89z_0)\left((0.20)^4-\frac{(0.20)^2}{3}-\frac{2}{3}\right)-(4.5z_0)^4(4.46z_0)\left((0.22)^4-\frac{(0.22)^2}{3}-\frac{2}{3}\right)\right]-$$

$$\frac{5}{128\times7}\left[(5z_0)^6(4.89z_0)\left((0.20)^6-\frac{(0.20)^4}{5}-\frac{4(0.20)^2}{15}-\frac{8}{15}\right)-(4.5z_0)^6(4.46z_0)\left((0.22)^6-\frac{(0.22)^4}{5}-\frac{4(0.22)^2}{15}-\frac{8}{21}\right)\right]$$

$$= 1.91z_0^3-103.67z_0^5-49.41z_0^5+1154.48z_0^7-561.80z_0^7$$

Therefore Y1+Y2 is given by

$$\frac{Y1+Y2}{2} = 1.91z_0^3-87.96z_0^5+519.65z_0^7 \qquad \text{(c)}$$

Since I_1 is given by

$$I_1 = \frac{Y1+Y2}{2}+Z$$

Then,

$$I_1 = 2.02z_0^3-87.96z_0^5+519.65z_0^7$$

We can see that since the expansion is valid for $z_0 \ll 1$, I_1 will be positive definite for any value of $z_0 < 0.46$ and at

$z_0 \simeq 0.46$, $I_1=0$.

We shall now evaluate coeficient I_2 .

For n=2.

$$Z = 2\left[z_0\left(y_0^2-1\right)^{1/2} - z_0\left(r_0^2-1\right)^{1/2}\right]\frac{1}{64}z_0^4$$

Using again the same values of the distribution function as in the case of n=1 we obtain,

$$Z = 0.013\, z_0^5 \qquad (a)$$

$$Y1 = \frac{1}{2}\int_{z_0 r_0}^{z_0 y_0}\left(J_1^2(z) - J_2^2(z)\right)\left(z_0^2 y_0^2 - z^2\right)^{1/2} z\,dz$$

$$= \frac{1}{2}\left\{\int_{z_0 r_0}^{z_0 y_0}\left(\frac{1}{4}z^2 - \frac{1}{16}z^4 - \frac{1}{64}z^4\right)\left(z_0^2 y_0^2 - z^2\right)^{1/2} z\,dz\right\}$$

$$= \frac{1}{2}\int_{z_0 r_0}^{z_0 y_0}\left(\frac{z^3}{4} - \frac{5}{64}z^5\right)\left(z_0^2 y_0^2 - z^2\right)^{1/2} dz$$

$$\therefore Y1 = \frac{1}{2}\left\{-\frac{1}{20}z_0^5 y_0^4\left(y_0^2 - r_0^2\right)^{1/2}\left[\left(\frac{r_0}{y_0}\right)^4 - \frac{1}{3}\left(\frac{r_0}{y_0}\right)^2 - \frac{2}{3}\right] + \right.$$

$$\left.\frac{5}{64\times 7}z_0^7 y_0^6\left(y_0^2 - r_0^2\right)^{1/2}\left[\left(\frac{r_0}{y_0}\right)^6 - \frac{1}{5}\left(\frac{r_0}{y_0}\right)^4 - \frac{4}{15}\left(\frac{r_0}{y_0}\right)^2 - \frac{8}{15}\right]\right\} \qquad (b)$$

$$Y2 = \frac{1}{2}\int_{z_0}^{z_0 r_0}\left(J_1^2(z) - J_2^2(z)\right)\left[\left(z_0^2 y_0^2 - z^2\right)^{1/2} - \left(z_0^2 r_0^2 - z^2\right)^{1/2}\right] z\,dz$$

$$= \frac{1}{2}\int_{z_0}^{z_0 r_0}\left(\frac{z^3}{4} - \frac{5}{64}z^5\right)\left[\left(z_0^2 y_0^2 - z^2\right)^{1/2} - \left(z_0^2 r_0^2 - z^2\right)^{1/2}\right] dz$$

$$\therefore Y2 = \frac{1}{2}\left\{\frac{1}{20}z_0^5 y_0^4\left(y_0^2 - r_0^2\right)^{1/2}\left[\left(\frac{r_0}{y_0}\right)^4 - \frac{1}{3}\left(\frac{r_0}{y_0}\right)^2 - \frac{2}{3}\right] - \right.$$

$$\frac{1}{20}\mathfrak{z}_0^5 y_0^4 (y_0^2-1)^{1/2}\left[\left(\frac{1}{y_0}\right)^4 - \frac{1}{3}\left(\frac{1}{y_0}\right)^2 - \frac{2}{3}\right] +$$

$$\frac{1}{20}\mathfrak{z}_0^5 r_0^4 (r_0^2-1)^{1/2}\left[r_0^4 - \frac{1}{3}r_0^2 - \frac{2}{3}\right] -$$

$$\frac{5}{64\times 7}\left\{\mathfrak{z}_0^7 y_0^6 (y_0^2-r_0^2)^{1/2}\left[\left(\frac{r_0}{y_0}\right)^6 - \frac{1}{5}\left(\frac{r_0}{y_0}\right)^4 - \frac{4}{15}\left(\frac{r_0}{y_0}\right)^2 - \frac{8}{15}\right] -\right.$$

$$\mathfrak{z}_0^7 y_0^6 (y_0^2-1)^{1/2}\left[\left(\frac{1}{y_0}\right)^6 - \frac{1}{5}\left(\frac{1}{y_0}\right)^4 - \frac{4}{15}\left(\frac{1}{y_0}\right)^2 - \frac{8}{15}\right] +$$

$$\left.\mathfrak{z}_0^7 r_0^6 (r_0^2-1)^{1/2}\left[\left(\frac{1}{r_0}\right)^6 - \frac{1}{5}\left(\frac{1}{r_0}\right)^4 - \frac{4}{15}\left(\frac{1}{r_0}\right)^2 - \frac{8}{15}\right]\right\}\Bigg\}$$

Y1 cancels out the first terms of the lines 1 and 4 and consequently Y1+Y2 is given by:

$$Y1+Y2 = -\frac{1}{40}\mathfrak{z}_0^5 y_0^4 (y_0^2-1)^{1/2}\left[\left(\frac{1}{y_0}\right)^4 - \frac{1}{3}\left(\frac{1}{y_0}\right)^2 - \frac{2}{3}\right] +$$

$$\frac{1}{40}\mathfrak{z}_0^5 r_0^4 (r_0^2-1)^{1/2}\left[r_0^4 - \frac{1}{3}r_0^2 - \frac{2}{3}\right] +$$

$$\frac{5}{128\times 7}\mathfrak{z}_0^7 y_0^6 (y_0^2-1)^{1/2}\left[\left(\frac{1}{y_0}\right)^6 - \frac{1}{5}\left(\frac{1}{y_0}\right)^4 - \frac{4}{15}\left(\frac{1}{y_0}\right)^2 - \frac{8}{15}\right] -$$

$$\frac{5}{128\times 7}\mathfrak{z}_0^7 r_0^6 (r_0^2-1)^{1/2}\left[\left(\frac{1}{r_0}\right)^6 - \frac{1}{5}\left(\frac{1}{r_0}\right)^4 - \frac{4}{15}\left(\frac{1}{r_0}\right)^2 - \frac{8}{15}\right]$$

Substituting for the values of the distribution function we obtain,

$$Y1+Y2 = -\frac{1}{40}(5\mathfrak{z}_0)^4(4.89\mathfrak{z}_0)\left(0.24^4 - \frac{1}{3}(0.20)^2 - \frac{2}{3}\right) +$$

$$\frac{1}{40}(4.5\mathfrak{z}_0)^4(4.46\mathfrak{z}_0)\left(0.22^4 - \frac{1}{3}(0.22)^2 - \frac{2}{3}\right) +$$

$$\frac{5}{128\times 7}\left(5z_0\right)^6\left(4.89z_0\right)\left(0.20^6 - \frac{1}{5}(0.20)^4 - \frac{4}{15}(0.20)^2 - \frac{8}{15}\right) -$$

$$\frac{5}{128\times 7}\left(4.5z_0\right)^6\left(4.46z_0\right)\left(0.22^6 - \frac{1}{5}(0.22)^4 - \frac{4}{15}(0.22)^2 - \frac{8}{15}\right)$$

$$Y1+Y2 = z_0^5(51.834) - z_0^5(24.705) - z_0^7(1154.48) + z_0^7(561.804)$$

Therefore,

$$\frac{Y1+Y2}{2} = 39.98z_0^5 - 519.65z_0^7 \qquad (c)$$

Since I_1 is given by

$$I_2 = Z + \frac{1}{2}\left(Y1+Y2\right)$$

Then,

$$I_2 = 39.99z_0^5 - 519.65z_0^7$$

Since the expansion is valid for $z_0 \ll 1$, I_2 will be positive definite for any value of $z_0 < 0.28$ and zero for $z_0 \simeq 0.28$. Therefore $I_1 I_2 > 0$ for $z_0 \ll 0.3$.

APPENDIX II.

Case of $k_\perp \to \infty$

By using equation (II. 4) the dispersion relation can be written as,

$$\mathcal{D}(\omega,k_\perp) \equiv 1 - \frac{3\omega_p^2}{2k_\perp^2}\frac{1}{(V_2-V_1)^3}\sum_{n=1}^{\infty}\frac{n\Omega}{\omega-n\Omega}\Bigg[J_n^2(k_\perp V_0/\Omega)\Big[(V_2^2-V_0^2)^{1/2}-(V_1^2-V_0^2)^{1/2}\Big] + \int_{V_1}^{V_2}\frac{\partial}{\partial v_\perp}\left(J_n^2(k_\perp v_\perp/\Omega)\right)(V_2^2-v_\perp^2)^{1/2}dv_\perp$$

$$+\int_{V_0}^{V_1}\frac{\partial}{\partial v_\perp}\left(J_n^2(k_\perp v_\perp/\Omega)\right)\Big[(V_2^2-v_\perp^2)^{1/2}-(V_1^2-v_\perp^2)^{1/2}\Big]dv_\perp\Bigg] \qquad (1)$$

Since the first integral in the above expression cancels the contribution of the second integral at V_1, the dispersion relation can be written as:

$$\mathcal{D}(\omega,k_\perp) \equiv 1 - \frac{3\omega_p^2}{2k_\perp^2}\frac{1}{(V_2-V_1)^3}\sum_{n=1}^{\infty}\frac{n\Omega}{\omega-n\Omega}\Bigg[J_n^2(k_\perp V_0/\Omega)\Big[(V_2^2-V_0^2)^{1/2}-(V_1^2-V_0^2)^{1/2}\Big] + \int_{V_0}^{V_2}\frac{\partial}{\partial v_\perp}\left(J_n^2(k_\perp v_\perp/\Omega)\right)(V_2^2-v_\perp^2)^{1/2}dv_\perp$$

$$-\int_{V_0}^{V_1}\frac{\partial}{\partial v_\perp}\left(J_n^2(k_\perp v_\perp/\Omega)\right)(V_1^2-v_\perp^2)^{1/2}dv_\perp\Bigg] \qquad (2)$$

Bessel functions of the first kind, of argument z and integral order n, can be approximated by the following expression

$$J_n(z) \simeq \sqrt{\left(\frac{2}{\pi z}\right)} \cos\left(z - \frac{n\pi}{2} - \frac{\pi}{4}\right) \qquad (3)$$

provided $z \to \infty$.

Consider now the first term in the summation of equation (2) above

$$J_n^2\left(k_\perp V_0/\Omega\right)\left[\left(V_2^2 - V_0^2\right)^{1/2} - \left(V_1^2 - V_0^2\right)^{1/2}\right]$$

by using expression (3), it can be written as

$$\frac{2}{\pi}\,\frac{\Omega}{k_\perp V_0} \cos^2\left(\frac{k_\perp V_0}{\Omega} - \frac{n\pi}{2} - \frac{\pi}{4}\right) \qquad (4)$$

It can be seen that the above term tends to zero as $k_\perp \to \infty$, whatever the value of n.

Consider now the integral

$$\int_{V_0}^{V} \frac{\partial}{\partial v_\perp}\left(J_n^2\left(k_\perp v_\perp/\Omega\right)\right)\left(V^2 - v_\perp^2\right)^{1/2} dv_\perp \qquad (5)$$

$$\simeq \int_{V_0}^{V} \frac{\partial}{\partial v_\perp}\left[\frac{2}{\pi}\,\frac{\Omega}{k_\perp v_\perp} \cos^2\left(k_\perp v_\perp/\Omega - \frac{n\pi}{2} - \frac{\pi}{4}\right)\right]\left(V^2 - v_\perp^2\right)^{1/2} dv_\perp$$

$$\simeq \int_{V_0}^{V} \frac{2}{\pi}\,\frac{\Omega}{k_\perp}\left[-\frac{1}{v_\perp^2} \cos^2\left(k_\perp v_\perp/\Omega - \frac{n\pi}{2} - \frac{\pi}{4}\right)\right.$$

$$\left. - \frac{2}{v_\perp} \cos\left(k_\perp v_\perp/\Omega - \frac{n\pi}{2} - \frac{\pi}{4}\right) \sin\left(\frac{k_\perp v_\perp}{\Omega} - \frac{n\pi}{2} - \frac{\pi}{4}\right)\frac{k_\perp}{\Omega}\right]\left(V^2 - v_\perp^2\right)^{1/2} dv_\perp$$

As $k_\perp \to \infty$ first term inside the above integral tends to zero.

Term (5) therefore becomes equal to

$$-\int_{V_o}^{V} \frac{2}{\pi}\frac{1}{v_\perp}\sin 2\left(\frac{k_\perp v_\perp}{\Omega} - \frac{n\pi}{2} - \frac{\pi}{4}\right)\left(V^2 - v_\perp^2\right)^{1/2} dv_\perp \qquad (6)$$

By using the trigonometric relation

$$\sin(A-B) = \sin A\cos B -- \sin B\cos A$$

in expression (6), we obtain for n=1 the following

$$-\int_{V_o}^{V} \frac{2}{\pi}\frac{1}{v_\perp}\left[-\cos\frac{\pi}{2}\sin\frac{2k_\perp v_\perp}{\Omega} + \sin\frac{\pi}{2}\cos\frac{2k_\perp v_\perp}{\Omega}\right]\left(V^2 - v_\perp^2\right)^{1/2} dv_\perp$$

$$= -\frac{2}{\pi}\int_{V_o}^{V} \frac{1}{v_\perp}\cos\frac{2k_\perp v_\perp}{\Omega}\left(V^2 - v_\perp^2\right)^{1/2} dv_\perp$$

and for n=2

$$-\int_{V_o}^{V} \frac{2}{\pi}\frac{1}{v_\perp}\left[\cos\frac{\pi}{2}\sin\frac{2k_\perp v_\perp}{\Omega} - \sin\frac{\pi}{2}\cos\frac{2k_\perp v_\perp}{\Omega}\right]\left(V^2 - v_\perp^2\right)^{1/2} dv_\perp$$

$$= \frac{2}{\pi}\int_{V_o}^{V} \frac{1}{v_\perp}\cos\frac{2k_\perp v_\perp}{\Omega}\left(V^2 - v_\perp^2\right)^{1/2} dv_\perp$$

In order to integrate the above expressions, we rewrite the cosine as a series expansion and rearranging we obtain, for n=1

$$\sum_{m=1}^{\infty}\left[\frac{2}{\pi}(-1)^m\left(\frac{2k_\perp}{\Omega}\right)^{2(m-1)}\int_{V_o}^{V} v_\perp^{2m-3}\left(V^2 - v_\perp^2\right)^{1/2} dv_\perp\right]\frac{1}{(2m-2)!} \qquad (7)$$

and for n=2

$$\sum_{m=1}^{\infty}\left[\frac{2}{\pi}(-1)^{m+1}\left(\frac{2k_\perp}{\Omega}\right)^{2(m-1)}\int_{V_o}^{V} v_\perp^{2m-3}\left(V^2 - v_\perp^2\right)^{1/2} dv_\perp\right]\frac{1}{(2m-2)!} \qquad (8)$$

In general therefore term (5) can be written as

$$\sum_{m=1}^{\infty} \frac{2}{\pi} (-1)^{m+(n-1)} \frac{1}{(2m-2)!} \left(\frac{2k_\perp}{\Omega}\right)^{2(m-1)} \int_{V_0}^{V} v_\perp^{2m-3} \left(V^2 - v_\perp^2\right)^{1/2} dv_\perp \qquad (9)$$

The Bessel function coefficient, I_n, is therefore given by

$$I_n = (-1)^{n-1} \sum_{m=1}^{\infty} \left[(-1)^m \left(\frac{2k_\perp}{\Omega}\right)^{2(m-1)}\right] \left[\int_{V_0}^{V_2} v_\perp^{2m-3} \left(V_2^2 - v_\perp^2\right)^{1/2} dv_\perp - \int_{V_0}^{V_1} v_\perp^{2m-3} \left(V_1^2 - v_\perp^2\right)^{1/2} dv_\perp \right] \frac{1}{(2m-2)!} \qquad (10)$$

From expression (10), above, it can be seen that $I_1 I_2 < 0$, that $\sum_{n=1}^{\infty} I_n$ is an oscillating series and that $\sum_{n=1}^{\infty} \frac{1}{W-n} I_n \to 0$.

REFERENCES

Baldwin,D.E. et al, Advances in Plasma Physics, Volume 3, ed. Simon and Thompson, Interscience, N.Y.,1969.

Bernstein, I., Waves in a Plasma in a Magnetic Field, Phys. Rev., 109, 10(1958).

Clemmow, P.C. and Dougherty, J.P., Electrodynamics of Particles and Plasmas, Addison-Wesley(1969).

De Forest, S.E. and McIlwain, C.E., J.G.R., 76, 3587(1971).

Dungey, J.W., Phys. Rev. Letters 6, 47(1961).

Evans, D.S., Aurora and Airglow 1968, B.M. McCormac, Reinhold, N.Y., 1969.

Frank, L.A., J.G.R., 72, 3753(1967b).

Fredricks, R., J.G.R., 76, 5344(1971).

Fritz, J.A. and Gurnett, D.A., J.G.R., 70, 2485(1965).

Gross, E.P., Phys. Rev., 82, 232(1951).

Harris, E.G., Physics Rev. Letters, 2, 34(1959).

Harris, E.G., J. N. Energy, C, 2, 138(1961).

Hones, E.W. et al , J.G.R., 72, 5879(1967).

Hones, E.W., Jr., et al, J.G.R., 76, 2977(1971b).

Hultqvist, B., Magnetospheric Physics, American Geophysical Union (1968).

Lezniak, T.W. and Winckler, J.R., J.G.R. 75, 7075(1970).

Nelms, G.L. and Lockwood G.E.K., Space Res., 7, 604(1966).

Ness, N.F., Magnetospheric Physics, American Geophysical Union,(1968).

Oya, H., J.G.R., 75, 4279(1970).

Oya, H., Phys. Fluids, 14, 2487(1971).

Pilkington, G.R., Earths Magnetospheric Processes, Ed. B. M. McCormac, D. Reidel, Holland(1972).

Post, R. F. and Rosenbluth, M.N., Phys. Fluids, 9, 730(1966).

Rosenbluth, M.N. and Post, R.F., Phys. Fluids, 8, 547(1965).

Scarf, F.L. and Fredricks, R.W., Report No. 99994-6075-RO-00

Scarf, F.L. and Fredricks, R.W., Earths Magnetospheric Processes, Ed. B.M. McCormac, D. Reidel, Holland(1972).

Scarf, F.W. and Fredricks, R.W., J.G.R., 78, 310(1973).

Stix, T.H., The Theory of Plasma Waves, The Advanced Physics Monograph Series, McGraw-Hill, N.Y.(1962).

Tataronis, J.A. and Crawford, F.W., Journal of Plasma Phys., 4, 231(1970).

Van Allen, J.A., Magnetospheric Physics, American Geophysical Union (1968).

Vette, J.I., Earth's Magnetospheric Processes, Ed. B.M. McCormac, D. Reidel, Holland (1972).

Young, T.S.T., Cullen, J.D. and McCune, J.E., Phys. Fluids, 14, 2783(1971).